**TITLE**

# Cyclin D1·Cdk4 regulates neuronal activity through phosphorylation of $GABA_A$ receptors

**AUTHORS**

Neus Pedraza*[#1], Ma Ventura Monserrat[#1], Francisco Ferrezuelo[1], Jordi Torres-Rosell[1], Neus Colomina[1], David Soto[2], Federico Miguez-Cabello[2], José A. Esteban[3], Joaquim Egea[4], Eloi Garí*[1].

[1]Cell Cycle, Department of Basic Medical Sciences, Institut de Recerca Biomèdica de Lleida (IRBLLEIDA), University of Lleida, Lleida, Spain.

[2]Institut d'Investigacions Biomèdiques August Pi i Sunyer (IDIBAPS), Hospital Clínic, Universitat de Barcelona, Barcelona, Spain. Laboratori de Neurofisiologia, Departament de Biomedicina, Facultat de Medicina i Ciències de la Salut, Institut de Neurociències, Universitat de Barcelona, Barcelona, Spain.

[3]Department of Molecular Neurobiology, Centro de Biología Molecular 'Severo Ochoa', Consejo Superior de Investigaciones Científicas (CSIC)/Universidad Autónoma de Madrid (UAM), Spain.

[4]Molecular and Developmental Neurobiology, Dept. Ciències Mèdiques Bàsiques, Facultat de Medicina, Universitat de Lleida/IRBLLEIDA, Rovira Roure 80, 25198, Lleida, Spain.

*Corresponding authors

[#]Co-authors

**ABSTRACT**

Cyclin D1 (Ccnd1)·Cdk4 complexes drive cell cycle progression through phosphorylation of pRb. Interestingly, Ccnd1 moves to the cytoplasm at the onset of differentiation in neuronal precursors. However, the cytoplasmic functions and targets of Ccnd1 in post-mitotic neurons are unknown. Here we identify the α4 subunit of gamma-aminobutyric acid (GABA) type A receptors ($GABA_ARs$) as an interactor and target of Ccnd1·Cdk4. Ccnd1 binds to an intracellular loop in α4 and, together with Cdk4, phosphorylates the α4 subunit at threonine 423 and serine 431. These modifications increase the activity of α4-containing $GABA_ARs$, measured in whole-cell patch-clamp recordings, and upregulate its surface levels. In agreement with this role of Ccnd1·Cdk4 in neuronal signaling, inhibition of Cdk4 decreases synaptic and extrasynaptic currents in the hippocampus of newborn rats. Moreover, *CCND1* knockout mice display an altered pattern of dendritic spines, according to α4 functions in synaptic pruning. Overall, our findings molecularly link Ccnd1·Cdk4 to $GABA_ARs$ activity in the central nervous system and highlight a novel role for this G1 cyclin in neuronal signaling.

Keywords: Cdk4/ Cyclin D1/ GABA signaling/ gamma-aminobutyric acid type A receptor subunit alpha4

## INTRODUCTION

Cyclin D1 (Ccnd1) and its catalytic counterparts, cyclin-dependent kinase 4 (Cdk4) and Cdk6, are main regulators of cell proliferation by promoting the G1-S phase transition of the cell cycle (reviewed in[1]). Under favorable conditions, mitogenic signals induce the expression of Ccnd1, the formation of Ccnd1·Cdk4/6 complexes and their localization to the nucleus. There, they phosphorylate the Retinoblastoma repressor protein (pRB), which eventually leads to its inhibition and in turn releases the activity of the E2F transcription factor. This induces the expression of genes required to go through the next steps of the cell cycle. This pRB-dependent control of cell proliferation is considered the "canonical" function of Ccnd1 and it has been reported as very relevant in tumor proliferation. Accordingly, Ccnd1 is classified as an oncogene frequently amplified in many types of neoplasia, and different cancer treatments with Cdk4/6 inhibitors such as Palbociclib have been approved to block this function. However, Ccnd1 also operates through several other non-canonical pathways including some pRB- and Cdk-independent ones to regulate different cellular processes (reviewed in[2]). Thus, Ccnd1 promotes cell detachment, migration and invasion of normal and tumor cells independently of pRB status[3],[4],[5] by interacting with cytoplasmic and membranous targets such as filamin A, pacsin, RalGTPases and paxillin[6],[7],[8],[9]. For example, Ccnd1·Cdk4 promotes cell invasion and metastasis through the phosphorylation of paxillin and the activation of the Rac1 pathway in membrane ruffles[9]. Moreover, the expression of a membrane-associated form of Ccnd1 harboring the pharnesylation signal of K-Ras (Ccnd1-CAAX) maximizes the ability of tumor cells to invade and metastasize[10]. Besides cell invasion, membrane-targeted Ccnd1 also influences cell-signaling responses[11].

The first hint for a role of Ccnd1 in the nervous system came from the analysis of *CCND1* knockout (KO) mice[12], which present certain behaviors (altered leg-clasping reflex) indicative of neurological abnormalities. Since then, several studies have substantiated the involvement of Ccnd1 in neuronal functioning. In neural stem cells, Ccnd1·Cdk4 has been involved in

regulating the length of G1, which is thought to influence the decision of cells to proliferate or differentiate[13],[14],[15]. Also, under pathological conditions, nuclear Ccnd1 reactivation/ upregulation in post-mitotic neurons has been observed to promote apoptosis (reviewed in[2]). Ccnd1 is located in the cytoplasm of differentiating post-mitotic cortical neurons and in neuroblastoma cell lines, although this has been proposed as a mechanism to prevent apoptosis[16] or to promote cell cycle withdrawal[17], respectively. Nevertheless, Ccnd1 could be exerting an active role in the cytoplasm. Interestingly, Ccnd1 is necessary for NGF-induced neuritogenesis in PC12 pheochromocytoma cell line[18]. Also cytoplasmic expression of Ccnd1·Cdk4 has been observed in the hippocampus during development[19] where it has been involved in neuronal plasticity[20]. But despite these works, the role and target/s of Ccnd1 in the nervous system and in particular its role in the cytoplasm of the neurons remains poorly understood.

γ-aminobutyric acid (GABA) is the major inhibitor neurotransmitter in the central nervous system. Its actions are mediated through different types of GABA receptors: GABA A receptors ($GABA_A$Rs), which are ligand-gated chloride ion channels, and GABA B receptors (metabotropic G-protein-coupled). Deficits in $GABA_A$R function are increasingly being involved in different pathologies, such as anxiety, cognitive deficits, depression, epilepsy, schizophrenia and substance abuse[21]. These receptors are also clinically relevant drug targets for anesthetic, anticonvulsant, anxiolytic, or sedative-hypnotic agents. $GABA_A$Rs mediate both phasic and tonic inhibition: synaptic $GABA_A$Rs are activated transiently by the GABA released from presynaptic vesicles, whereas extrasynaptic $GABA_A$Rs are activated by low GABA concentrations in the extracellular space and thus mediate tonic inhibition. The tonic inhibitory currents control neuronal excitability and the strength of synaptic transmission[22].

$GABA_A$Rs are heteropentamers that belong to the ligand-gated ion channel superfamily. A total of 19 subunits (as well as splice variants) have been cloned and grouped into eight subunit classes: α (1-6), β (1-3), γ (1-3), δ, ε, π, θ and ρ (1-3). $GABA_A$Rs are usually formed by two α, two

β, and one γ or one δ subunits. Each subunit contains a large amino-terminal extracellular
92 domain and four transmembrane (TM) domains. Between TM3 and TM4 there is a large intracellular loop (ICL) where regulation by phosphorylation and protein interactions primarily
94 occurs. The subunit composition dictates its subcellular location and function.

$GABA_A$Rs containing the α4 subunit are expressed in the hippocampus, cortex and thalamus,
96 and mediate extrasynaptic inhibition in thalamus and dentate gyrus[23]. At the onset of puberty, α4-β-δ $GABA_A$R expression increases perisynaptically at excitatory synapses in the
98 hippocampus, contributing to anxiety, synaptic pruning and learning deficits in mice[24],[25],[26],[27],[28]. In fact, in the α4-KO mice synaptic pruning is prevented, and
100 synaptic plasticity and learning abilities are restored[23],[29],[30]. In the adult hippocampal neurogenesis, α4-containing $GABA_A$Rs are involved in proliferation, migration and dendritic
102 development[31]. Mutations in the GABAergic receptor subunit 4 gene *GABRA4*[32],[33],[34] and reduced protein and mRNA levels of α4[35],[36] are reported in patients of autism
104 spectrum disorder. Furthermore, the α4-KO mice show a phenotype compatible with high-functioning autism[37].

106 Here we report that Ccnd1 interacts with the α4 subunit of $GABA_A$Rs. Ccnd1·Cdk4 complex phosphorylates α4 in the intracellular loop between TM3 and TM4 and enhances the efficacy
108 of α4-containing $GABA_A$Rs, affecting the pattern of dendritic spines. We propose a novel role for cytoplasmic Ccnd1·Cdk4/6 in regulating α4-containing $GABA_A$Rs in the central nervous
110 system.

## 112 RESULTS

### The α4 subunit of $GABA_A$ receptors interacts with cyclin D1

114 To investigate the role of Ccnd1 in the nervous system, we performed a yeast two-hybrid screening using Ccnd1 as a bait and an adult mouse brain library as a prey[38]. We found that
116 Ccnd1 interacts with the C-terminal half of the α4 $GABA_A$R subunit (Gabra4). We obtained

three independent clones spanning amino acids 354-552, 385-552 and 386-552 (Fig 1A). This
118 region of α4 contains the intracellular loop (ICL) between the TM3 and TM4 transmembrane domains, which is phosphorylated by protein kinase C (PKC,[39]). To confirm the interaction
120 between the α4 subunit and Ccnd1 we carried out immunoprecipitation (IP) experiments with FLAG-tagged Ccnd1 and the HA-tagged C-terminal region of α4 (354-552aa) expressed in HEK-
122 293T cells. We observed specific co-IP of the C-terminal domain of α4 in the Ccnd1 IP (Fig 1B). To test whether there is a direct interaction between Ccnd1 and the α4 subunit, we performed
124 *in vitro* GST-pull-down assays. Fusions of GST-α4 or GST-C-terminal α4 (354-552aa) purified from *E.coli* were mixed with FLAG-Ccnd1 produced by *in vitro* transcription and translation.
126 Ccnd1 was co-precipitated when GST-α4 or GST-C-terminal α4 were pulled down, but not with GST alone (Fig 1C). To analyze the endogenous interaction between Ccnd1 and the α4 $GABA_AR$
128 subunit, we immunoprecipitated Ccnd1 from the hippocampus of adult mice, since co-expression of Ccnd1 and α4 mRNAs in the CA1, CA3 and dentate gyrus regions of the
130 hippocampus is observed in the Allen mouse brain atlas (www.brain-map.org). As shown in figure 1D, α4 subunit of $GABA_AR$ co-immunoprecipitated with endogenous Ccnd1, in a specific
132 manner. Overall, our data indicate that there is a specific and direct interaction between Ccnd1 and the α4 subunit of $GABA_A$ receptors.

**Figure 1**

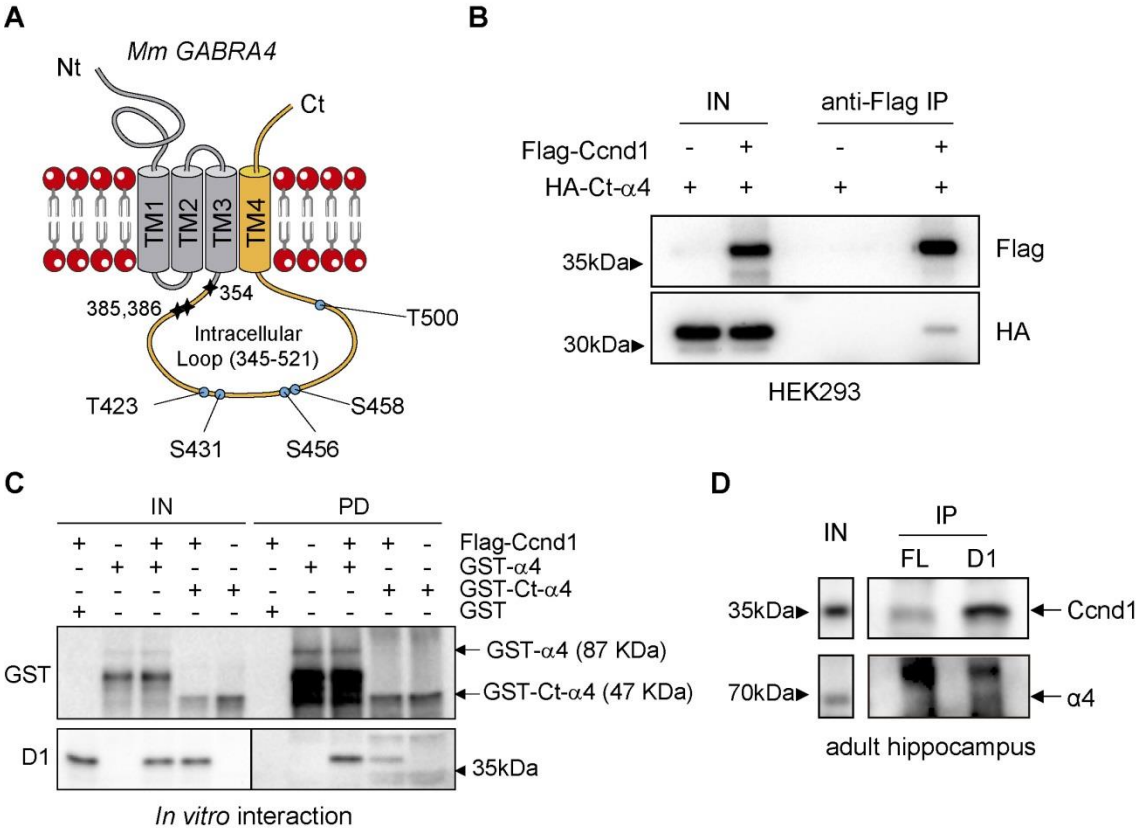


***Figure 1. Ccnd1 interacts with the α4 subunit of GABA$_A$ receptors.*** *A) Scheme representing the mouse α4 subunit of GABA$_A$Rs (552aa). N terminal (Nt) and C terminal (Ct), intracellular and extracellular domains and the four transmembrane domains (TM1-4) are shown. In a yeast two-hybrid screening, Ccnd1 was found to interact with three independent clones of the C-terminal region of the α4 subunit (in yellow), spanning amino acids 354-552, 385-552, 386-552 (the starting amino acids are shown as stars). The three clones contained the intracellular loop (ICL) between TM3 and TM4. Putative phosphorylation sites for Cdk (SP or TP) in the ICL are shown in blue. B) HEK-293T cells were transfected with the C terminus of α4 subunit (354-552aa, tagged with HA: HA-Ct-α4) and Ccnd1 (tagged with Flag: Flag-Ccnd1). Flag-Ccnd1 was precipitated using αFlag agarose beads (Sigma). Input (IN) and immunoprecipitation (IP) samples were analyzed by western blot using anti-HA and anti-Flag antibodies, to detect co-IP of the C terminus of α4 with Ccnd1. C) In vitro translated FLAG-Ccnd1 was incubated with recombinant GST or GST fusions of α4 full length (GST-α4) or the C terminus of α4 (GST-Ct-α4) purified from E. coli. Input (IN) and GST pull down (PD) samples were analyzed by western blot using anti-Flag antibody to detect Ccnd1 and anti-GST antibody to detect α4. Intact protein fusions are indicated. D) Immunoprecipitation of endogenous Ccnd1 from adult mouse hippocampal extracts was performed*

150 *using a rabbit polyclonal antibody against Ccnd1. As a control, a rabbit polyclonal antibody against the Flag epitope (FL) was used. Input (IN) and IP samples were analyzed by western blot to detect Ccnd1 and*
152 *α4 subunit.*

154 **The α4 subunit of $GABA_A$Rs is phosphorylated at T423 and S431 by Ccnd1·Cdk4 complex**

As Ccnd1 is the regulatory subunit of Cdk4/6 kinases, we analyzed the sequence of α4 for
156 putative phosphorylation sites by Cdks. We found five S/TP sites in the sequence of the intracellular loop (Fig 1A). In an *in vitro* kinase assay, Ccnd1·Cdk4 complex phosphorylated
158 recombinant GST-α4 and this phosphorylation was prevented by inhibiting the complex with the specific Cdk4/6 inhibitor Palbociclib (Fig 2A). Besides, another subunit of the $GABA_A$Rs, β3,
160 which lacks S/TP sites, was not phosphorylated by the Ccnd1·Cdk4 complex (Fig 2B). In order to know which residues of α4 were phosphorylated by Ccnd1·Cdk4, we mutated the five
162 intracellular putative Cdk phosphorylation sites to non-phosphorylatable residues (alanine) generating three different mutant alleles: T423A and S431A ($\alpha4^{T423AS431A}$); S456A and S458A
164 ($\alpha4^{S456AS458A}$); and T500A ($\alpha4^{T500A}$). Neither $\alpha4^{S456AS458A}$ nor $\alpha4^{T500A}$ mutants showed a decrease in phosphorylation by Ccnd1·Cdk4 (Fig 2C and 2D). However, the non-phosphorylatable mutant
166 of T423 and S431 ($\alpha4^{T423AS431A}$: AA) significantly reduced phosphorylation by Ccnd1·Cdk4 *in vitro*, either with the full-length or the C-terminus construct of α4 (Fig 2C-F). Moreover, we
168 analyzed by mass spectrometry phosphopeptides from the C-terminus of α4 subunit phosphorylated by Ccnd1·Cdk4, and we found that both T423 and S431 were phosphorylated
170 *in vitro* (S1 Table). Altogether, our results show that Ccnd1·Cdk4 complex is able to phosphorylate α4 subunit at T423 and S431.

172 To investigate if the α4 subunit is also phosphorylated by Ccnd1·Cdk *in vivo*, we immunoprecipitated Cdk substrates with an anti-phospho-Threonine-Proline (phosphoTP)
174 antibody and the presence of phosphorylated α4 was assessed by western blot. We transiently transfected HEK-293T cells with α4, β3 subunits and Ccnd1 or $Ccnd1^{K112E}$, a mutant of Ccnd1

176 that does not form an active complex with Cdk[40]. For the experiments where we co-expressed Ccnd1 or Ccnd1$^{K112E}$, we used a variant that contains the CAAX motif of K-ras to

178 maintain Ccnd1 attached to the cell membrane[10] to improve the phosphorylation of membrane targets. In the phosphoTP IP, we observed an increase in the phosphorylated α4

180 subunit in the presence of Ccnd1-CAAX relative to the presence of Ccnd1$^{K112E}$-CAAX (Fig 2G and 2H). Moreover, when we used the non-phosphorylatable α4 mutant (α4$^{T423AS431A}$: AA), we did

182 not observe higher levels of phosphorylated α4 in the presence of Ccnd1 (Fig 2G and 2H). This data suggests that Ccnd1·Cdk4 can phosphorylate α4 *in vivo* at least at T423.

## Figure 2

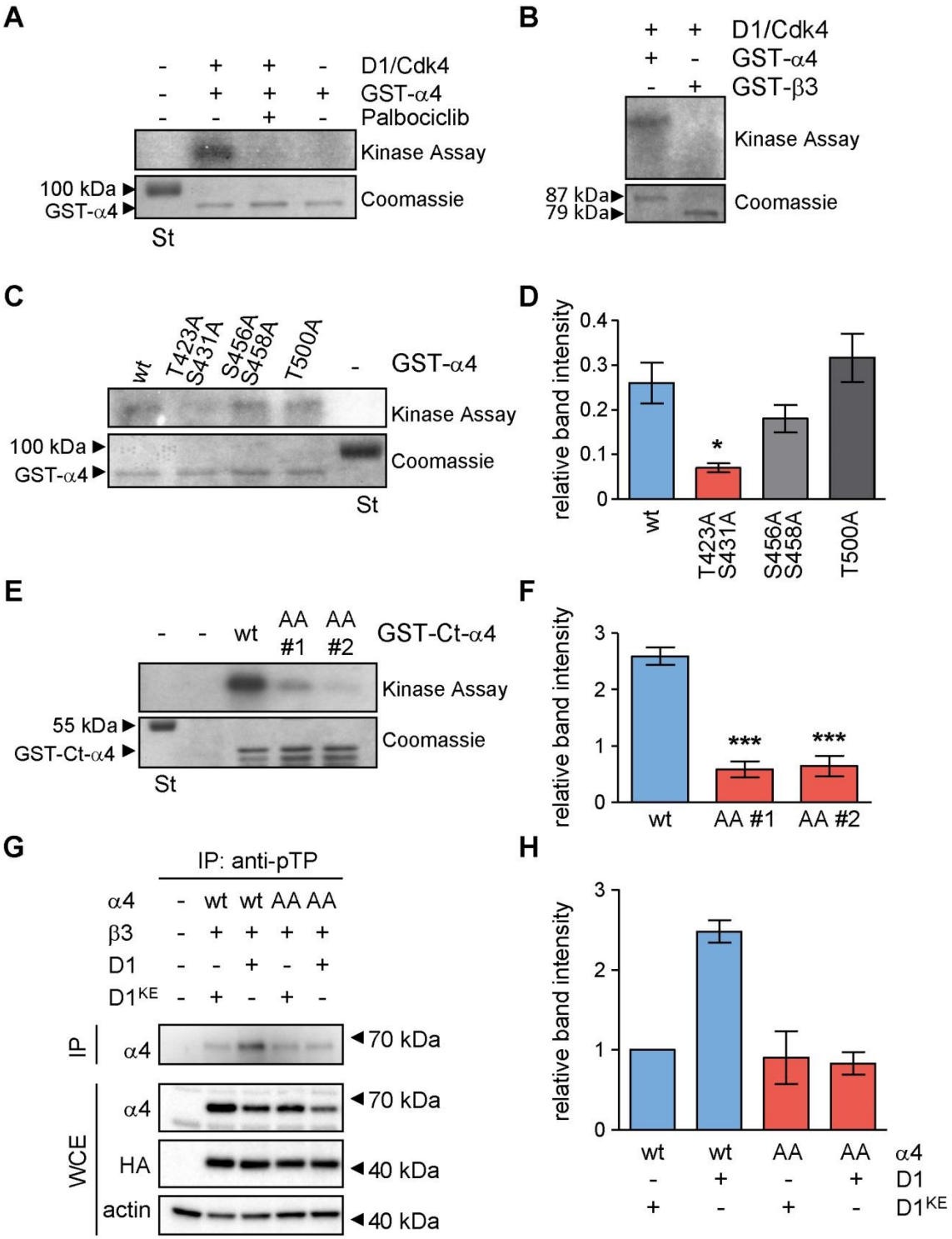


***Figure 2. Ccnd1·Cdk4 phosphorylates α4 at T423 and S431 residues.*** *A) In vitro radioactive kinase assay using purified recombinant GST-α4 fusion and Ccnd1·Cdk4 (Sigma). Cdk4/6 inhibitor Palbociclib was added at 1 μM concentration. Coomassie blue staining is shown as loading control (Input). B) Recombinant GST-α4 and GST-β3 fusions were tested for Ccnd1·Cdk4 kinase activity as in A. C) Kinase*

*assay was performed with Ccnd1·Cdk4 against GST-α4 wild type and the non phosphorylatable mutants:*
190 *T423A, S431A; S456A, S458A; and T500A. D) Quantification of the phosphorylation in C showing the mean ± S.E.M. The amount is relative to a pRB control (n=3, One-way ANOVA, post-Tukey analysis*
192 **p<0.05). E) Kinase assay was performed with Ccnd1·Cdk4 against the C-terminus of α4 wild type (GST-Ct-α4 wt) and two clones (#1 and #2) of the non phosphorylatable mutant T423A, S431A (AA). F)*
194 *Quantification of the phosphorylation in E showing the mean ± S.E.M. The amount is relative to a pRB control (n=3, ANOVA ***p<0.001). G) Immunoprecipitation of Cdk substrates in HEK-293T cells*
196 *transfected with α4 wild type (wt) or the non phosphorylatable mutant T423A, S431A (AA), together with β3 and HA-Ccnd1-CAAX (D1) or HA-Ccnd1$^{K112E}$-CAAX (D1$^{KE}$). PhosphoTP antibody was used for the*
198 *immunoprecipitation (IP), and α4 was detected by immunoblot. Protein levels of α4, Ccnd1 (anti-HA antibody) and actin were also analyzed in the whole cell extract (WCE). H) Quantification of the*
200 *phosphorylation in G showing the mean ± SD (n=2).*

202 **Ccnd1·Cdk4 promotes the activation of α4-containing GABA$_A$ receptors**

Because Ccnd1·Cdk4 phosphorylates the α4 subunit in the intracellular loop, we reasoned that
204 it may also affect the performance of α4-containing GABA$_A$Rs. To study the electrophysiology of GABA$_A$Rs we carried out whole cell patch-clamp recordings of HEK293 tsA201 cells
206 transiently expressing α4 and β3 subunits (Fig 3A), since functional GABA$_A$ receptors can be formed in HEK-293T cells by co-expression of these subunits[39]. To measure the behavior of
208 the α4β3 GABA$_A$Rs, 1 μM GABA was applied for 5 seconds every 2 min in these cells (Fig 3A and S1). Receptor-mediated current amplitude decreased (rundown) over time (Fig 3A and S1A):
210 after 12 minutes of recording, GABA-mediated current was 60 ± 5 % (n=7) of the initial response (Fig 3A and S1D). Co-expression of Ccnd1-CAAX with α4β3 receptors partially
212 prevented their rundown in a significant manner (Fig 3A and S1B). At 12 minutes after the start of the experiment, the GABA-mediated current amplitude, in the presence of Ccnd1-CAAX, was
214 80 ± 9 % (n=5) of the initial GABA-mediated response (Fig 3A and S1D). To confirm that phosphorylation of T423 S431 in α4 is important for this effect, we co-transfected a

216 phosphomimetic α4$^{T423ES431E}$ (α4$^{EE}$) mutant with β3 and observed that it completely obliterates the rundown of $GABA_A$Rs (Fig 3A and S1C). Thus, our data suggest that Ccnd1 can enhance the

218 efficacy of α4-containing $GABA_A$Rs by modulating the activity of the receptor through the phosphorylation of α4.

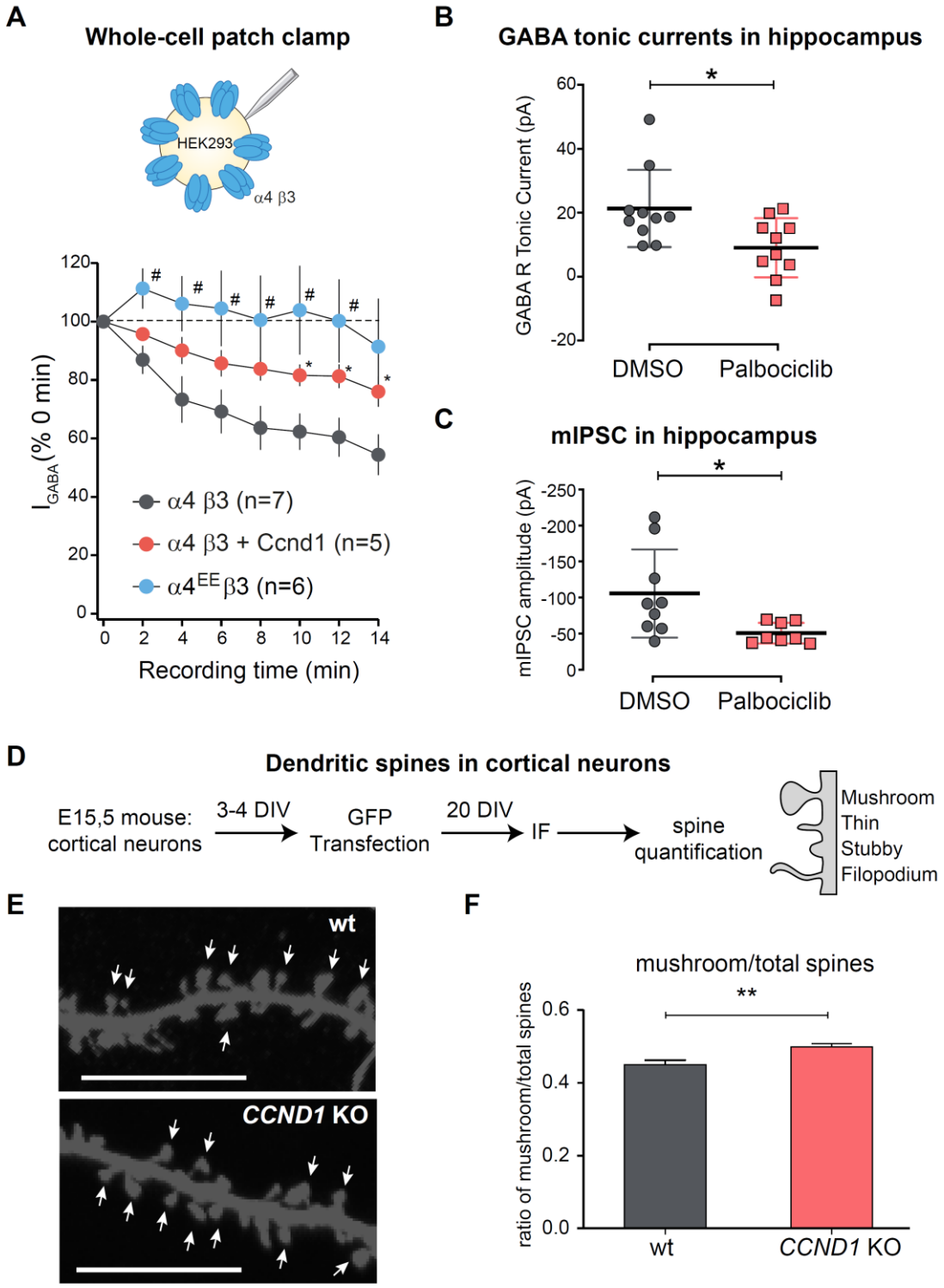


220

222 ***Figure 3. Ccnd1·Cdk4/6 modulates α4-containing GABA$_A$ receptor activity. A) Ccnd1 or the phosphomimetic allele of α4 (α4$^{EE}$) decreases GABA$_A$ receptor rundown.*** *Whole-cell patch clamp*
224 *configuration for GABA currents recording in HEK-tsA201 cells transfected with α4 and β3 subunits of GABA$_A$Rs. Currents were evoked by rapid application of 1 µM GABA and holding potential was held at*
226 *−60mV. Peak current values at different times of GABA stimulations were analyzed in cells under 3 conditions: 1) α4 wt (α4β3, grey circles), 2) α4 wt co-transfected with Ccnd1-CAAX (α4β3+Ccnd1, red*
228 *circles) and 3) α4$^{T423E\ S431E}$ phosphomimetic allele (α4$^{EE}$β3, blue circles). *p<0.05, α4β3 vs. α4β3+Ccnd1; #p<0.05 α4β3 vs. α4$^{EE}$β3; Unpaired student's t-Test.* ***B and C) Cdk4/6 inhibition by Palbociclib decreases***
230 ***GABA tonic currents and mIPSC amplitude in rat hippocampal slices.*** *GABA currents recordings in CA1 neurons: hippocampal slices from newborn rats were cultured in vitro, treated for 2 h with DMSO or*
232 *Palbociclib 2.5 µM, and tonic (extrasynaptic) or mIPSCs (synaptic currents) were measured. B) GABA inhibitory postsynaptic currents were evoked by stimulation of Schaffer collaterals and the tonic GABA$_A$*
234 *receptor-mediated current was measured as the outward shift in holding current following application of the GABA$_A$R antagonist picrotoxin. CA1 pyramidal neurons were recorded under whole-cell voltage-*
236 *clamp at -60 mV. Quantification of the shift in holding current for DMSO- and Palbociclib-treated cells (n=10), represented in a scatter dot plot showing mean values ± S.E.M (*p<0.05, Wilcoxon-Mann-*
238 *Whitney test). The shift in holding currents, corresponding to tonic currents, is reduced in Palbociclib-treated slices compared to vehicle. C) To measure miniature inhibitory postsynaptic currents (mIPSC), 1*
240 *µM tetrodotoxin was added to block action potentials. Scatter dot plot showing mIPSC amplitude quantifications of DMSO- (n=9) and Palbociclib-treated cells (n=8). Bars show mean values ± S.E.M.*
242 **p<0.05, Wilcoxon-Mann-Whitney test.* ***D-F) CCND1 KO increases the maturity of dendritic spines in cortical neurons****. D) Schematic representation of the experimental design for dendritic spine analysis of*
244 *cortical neurons at 20 DIV. Cultured cortical neurons from WT and CCND1 KO mice were transfected at 3 DIV with GFP and fixed at 20 DIV. Changes in spine density and morphology were assessed by analyzing*
246 *GFP-positive neurons with NeuronJ (see Materials and Methods). E) Confocal images of representative neurites from WT and CCND1 KO neurons are shown. Scale bar: 10 µm. F) Quantification of the number*
248 *of mushroom spines relative to the number of total spines from WT (n= 59 neurons) and CCND1 KO (n= 62) neurons (4 mice/group). Bars show mean values ± S.E.M. **p<0.01, Unpaired student's t-test.*

250

The α4 subunit is a component of extra-synaptic, high-affinity $GABA_A$Rs, which mediate tonic
252 inhibition. To assess the importance of Ccnd·Cdk4/6 on $GABA_A$Rs in a physiological context, we measured tonic currents in hippocampal slices of newborn rats. Organotypic hippocampal slice
254 cultures were treated with DMSO (vehicle) or the Cdk4/6 specific inhibitor Palbociclib at 2.5 µM for 2 h (Fig 3B and S2A). GABA inhibitory post synaptic currents were evoked with single
256 voltage pulses in Schaffer collaterals, and tonic currents were recorded from CA1 pyramidal neurons under whole-cell voltage-clamp configuration. The application of the antagonist
258 picrotoxin (100 µM) causes a decrease in the operative extra-synaptic $GABA_A$ channels, which can be measured as an outward shift of the holding current[41] (Fig S2B). This shift
260 corresponds to the $GABA_A$R tonic currents (Fig 3B). While the holding current in DMSO-treated cells was shifted by 21 ± 4 pA, the shift in Palbociclib-treated slices was only 9 ± 3 pA (Fig 3B).
262 Therefore, Ccnd·Cdk4/6 inhibition by acute Palbociclib application causes a significant decrease in the $GABA_A$R tonic current.

264 Given that the α4 subunit can also form synaptic receptors when clustered together with βxγ2 subunits[42], we tested whether the acute Cdk4/6 inhibition may in turn affect $GABA_A$
266 receptor synaptic function. To this end, we measured miniature inhibitory postsynaptic currents (mIPSC) in organotypic cultures treated with 2.5 µM Palbociclib for 2 h, in the
268 presence of the action potential blocker tetrodotoxin (1 µM) (Fig S2A). We observed that the amplitude of the spontaneous miniature responses was reduced after Ccnd·Cdk4/6 inhibitor
270 treatment as compared to the control (DMSO) treatment (-106 ± 20 pA for DMSO vs -51 ± 5 pA for Palbociclib; Fig 3C and S2C-D). Putting all these electrophysiological experiments together,
272 our results suggest that Ccnd1·Cdk4/6 enhances $GABA_A$R activity in the hippocampus.

Since Ccnd1 regulates α4-containing $GABA_A$ receptors, we asked if the absence of Ccnd1 could
274 disrupt some α4-dependent functions of $GABA_A$Rs *in vivo*. The α4 subunit of $GABA_A$Rs promotes synaptic pruning (the removal of dendritic spines) in the hippocampus of adolescent

276 mice[27],[28]. To assess whether Ccnd1 could affect normal dendritic spine development, we analyzed the number and morphology of dendritic spines in cortical neurons from WT and 278 *CCND1* KO mice. Cultured neurons were transfected with GFP at 3 DIV, and dendritic spines were analyzed at 20 DIV, when spines are completely developed (Fig 3D-F and S3). The density 280 of dendritic spines did not depend on Ccnd1 expression (WT= 8.51 ± 0.16 vs *CCND1* KO= 8.28 ± 0.18 spines/10 µm, non-significant, Fig S3B). However, the ratio of the mushroom-shape (more 282 mature) spines relative to total spines was significantly increased in *CCND1* KO neurons compared with neurons from WT animals (0.45 ± 0.01 vs 0.50 ± 0.01, $p<0.01$, Fig 3F). Overall, 284 our data suggest that Ccnd1·Cdk4/6 enhances α4-dependent $GABA_AR$ activity, which may have consequences for normal dendritic spine development.

286

**Ccnd1 increases the surface levels of the α4 subunit of $GABA_A$ receptors**

288 Phosphorylation of several subunits of $GABA_A$ receptors can affect their abundance at the cell surface, where they are active[43]. To analyze whether phosphorylation by Ccnd1·Cdk4 may 290 affect $GABA_AR$ localization, we studied the surface levels of the α4 subunit when co-expressed heterologously with Ccnd1 in HEK-293T cells. For this, we transiently expressed α4 and β3 in 292 these cells and assessed the surface levels of α4 by biotin labeling of surface proteins (Fig 4A). We used the transferrin receptor (TFRC) protein levels as a surface protein control and 294 quantified the levels of α4 at the surface relative to the levels of α4 in the total cell extract (Fig 4B). We observed a statistically significant increase in the surface levels of α4 (148 ± 20%, 296 P=0.04, Fig 4A and B) only when Ccnd1-CAAX was also co-expressed. This increase was abolished in the presence of $Ccnd1^{K112E}$-CAAX, as well as when the non-phosphorylatable 298 mutant $α4^{T423AS431A}$ was used (98 ± 29%, P=0.93 and 107 ± 24%, P=0.82, respectively), indicating that the observed effect depends on T423/S431 phosphorylation by Ccnd1·Cdk4. These results 300 suggest that Ccnd1 increases the surface levels of the α4 subunit of $GABA_AR$ in a kinase-dependent manner.

302

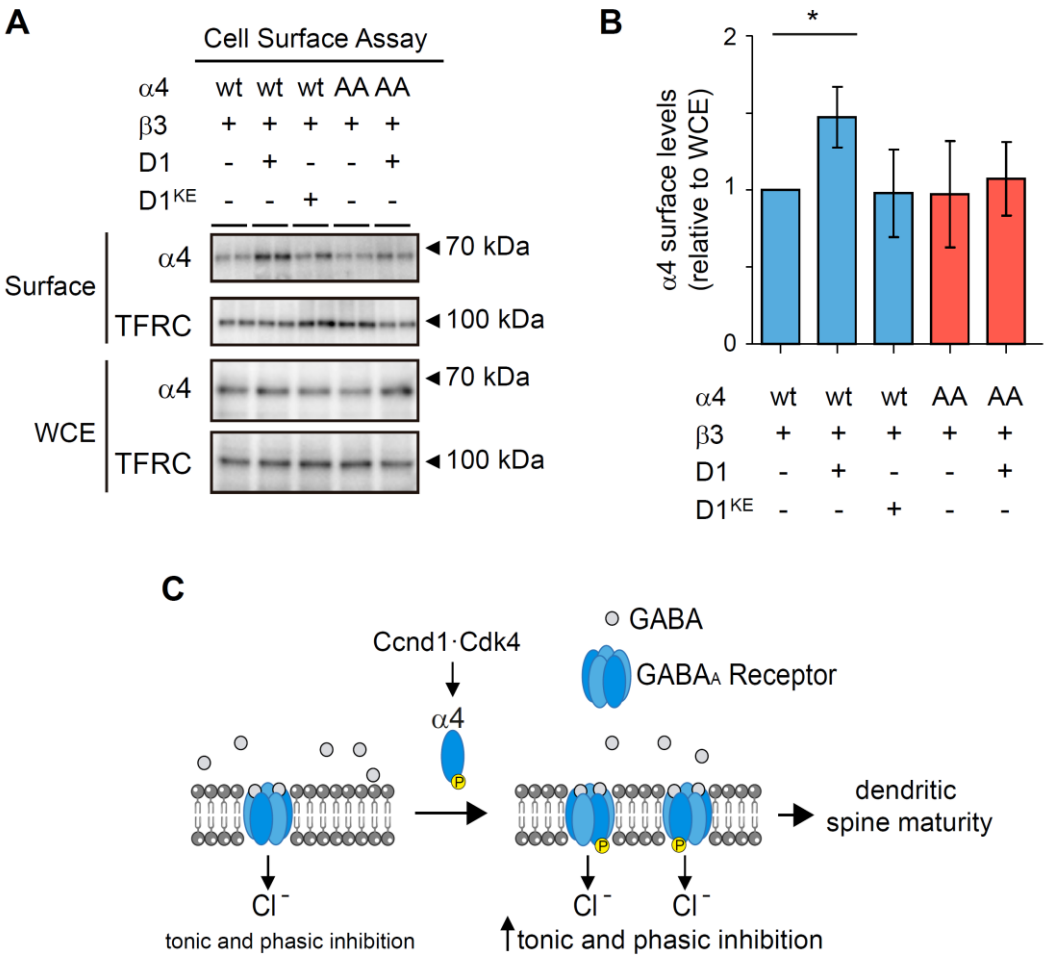


304 ***Figure 4. Ccnd1 increases surface levels of α4 subunit.*** *A) HEK-293T cells were transfected with β3 and α4-FLAG or the nonphosphorylatable mutant (α4$^{T42A3S431A}$-FLAG: AA). Either HA-Ccnd1-CAAX (D1) or HA-*

306 *Ccnd1$^{K112E}$-CAAX (D1$^{KE}$) or a control vector was co-transfected. A biotinylation assay was used to purify cell surface proteins. TFRC is used to normalize α4 levels. Representative blots with whole cell extracts*

308 *and surface proteins are shown. Antibodies used for protein detection are: polyclonal rabbit anti-FLAG to detect α4-FLAG; TFRC, monoclonal mouse anti-TFRC. B) Quantification of the experiment in A as a*

310 *surface to WCE ratio. Bars show mean values ± S.E.M (n=4 independent experiments). *p<0.05 (Unpaired student's t-test). C) Schematic model of the effects of Ccnd1·Cdk4 on α4-containing GABA$_A$ receptors:*

312 *Ccnd1·Cdk4 phosphorylates the α4 subunit, promoting its surface localization and activity, thus increasing synaptic (phasic) and extrasynaptic (tonic) inhibition and altering the maturity of dendritic*

314 *spines.*

316

**DISCUSSION**

318 In neurons, Ccnd1·Cdk4 has been involved in promoting proliferation versus differentiation of stem cells during cortical development[13] and in the adult hippocampus[44]. However, the 320 role of Ccnd1 in the regulation of neuronal signaling has never been investigated before. Interestingly, *CCND1* KO mice show an abnormal limb-clasping reflex[12], being this alteration 322 an early symptom of neurological defects associated with hippocampal neuron malfunctioning[45]. In this work, we have unveiled a novel role of Ccnd1 in the stimulation of 324 $GABA_A$ receptor function (Fig 4C). Ccnd1 interacts with the α4 subunit of $GABA_AR$ and Ccnd1·Cdk4 complex phosphorylates T423 and S431 in the intracellular loop of α4. This 326 phosphorylation increases the surface levels of α4 subunit and the efficacy of $GABA_AR$ activity in whole cell patch-clamp recordings. Furthermore, Ccnd·Cdk4/6 inhibition decreases tonic 328 currents and the amplitude of mIPSCs in the hippocampus of newborn rats. Accordingly, the proportion of mature dendritic spines is increased in cortical neurons from *CCND1* KO mice. 330 Therefore, we propose that Ccnd1·Cdk4 mediated phosphorylation is an important physiological regulator of $GABA_AR$-mediated inhibition.

332 Ccnd1 has been found in the cytoplasm of postmitotic neurons[16]. As nuclear localization of Ccnd1 in these cells promotes apoptosis, its cytoplasmic localization has been suggested as a 334 Ccnd1 sequestration mechanism to avoid cell death. However, Ccnd1·Cdk4 has cytoplasmic functions interacting with membrane-associated proteins such as Filamin A, RalGTPases and 336 Paxillin[6],[8],[9],[46]. It is then possible that Ccnd1·Cdk4 plays an active role in the cytoplasm of post-mitotic neurons. Supporting this, the mRNA of Ccnd1 has also been found in the 338 synaptic neuropil in the hippocampus[47], suggesting local translation of Ccnd1 in the dendrites. Also, Cdk4 has been localized in the cytoplasm in adolescent mouse hippocampal 340 neurons[20]. According with a hippocampal cytoplasmic expression of Ccnd1, here we have

detected co-immunoprecipitation of Ccnd1 and α4 in samples from mouse hippocampus where this subunit of the $GABA_AR$ is abundantly expressed[23], providing evidences for a cytoplasmic role of Ccnd1 in neurons.

In this work, we have proved that Ccnd1·Cdk4 phosphorylates α4 at T423 and S431 in the intracellular loop (ICL) *in vitro*. Moreover, in transiently transfected HEK-293T cells, we have detected Ccnd1-specific phosphorylation of α4 *in vivo*. Rundown of $GABA_A$ receptors involves phosphorylation-dephosphorylation processes[48],[49],[50]. The ICL between TM3 and TM4 of several subunits of $GABA_ARs$ is regulated by phosphorylation, affecting the interaction of $GABA_A$ receptors with other proteins, the stability and the surface localization of the subunits, or the activity of the $GABA_A$ receptors[21]. For instance, PKC phosphorylates the α4 subunit in the intracellular loop (S443) increasing its stability, membrane insertion and the efficacy of $GABA_ARs$[39],[51]. Consistent with these previous data, we have determined by whole-cell patch-clamp recordings that the expression of Ccnd1 or the phosphomimetic allele of α4 ($\alpha4^{T423ES431E}$) caused a decrease in the rundown of α4β3 containing $GABA_A$ receptors in HEK-293 cells. We propose that Ccnd1·Cdk4 enhances the activity of α4-containing $GABA_A$ receptors by promoting the surface accumulation of α4 through its phosphorylation. On the one hand, Ccnd1 but not the inactive allele $Ccnd1^{K112E}$ is able to promote surface accumulation of α4. Moreover, Ccnd1 does not increase surface levels of the non-phosphorylatable mutant of α4 ($\alpha4^{T423AS431A}$).

The adjustment of the surface levels of $GABA_AR$ subunits takes place through the regulation of export and internalization processes. The ICL of β3 subunit is involved in internalization of the receptors by clathrin. There is an atypical site for interaction with clathrin adaptor protein 2 (AP2) (KTHLRRRSSQLK), that contains the phosphorylation site for PKA, PKC and CamKII: it only binds AP2 when dephosphorylated[52]. Such a mechanism could also be happening for α4 subunit, that contains a similar motif (NMRKRTNAL) in the intracellular loop (aa 385-393). In fact, α4 has been described to interact directly with clathrin μ2 by immunoprecipitation[53].

Although T423 and S431 are not found inside the motif, phosphorylation of the ICL and/or the presence of Ccnd1 could be affecting the binding of α4 to clathrin. Another possibility is that the trafficking from the ER to the cytoplasmic membrane is affected. In the α4 and δ subunits there are dibasic or multibasic motifs in homologous positions that reduce export from the ER and increase transport back from the Golgi apparatus to the ER[54]. The mutation of dibasic motif to Ala in α4 enhances surface expression of the receptors. Again, phosphorylation of ICL or interaction with Ccnd1 could affect the association of dibasic sites with trafficking proteins.

Consistently with a role of Ccnd1·Cdk4/6 on GABAergic signaling, we have shown that inhibition of Cdk4/6 in CA1 pyramidal neurons produces a decrease in tonic currents and the amplitude of mIPSCs. Even though α4 is mostly extrasynaptical, it can also form synaptic $GABA_A$Rs when assembled with γ2. Concerning mIPSC amplitude, it is feasible that phosphorylation of α4 by Ccnd·Cdk4/6 complexes is still promoting its activity also when the α4 subunit is forming α4βxγ2 receptors at the synapse[55]. This would mean that α4 phosphorylation by Ccnd·Cdk4/6 has the same effect irrespective of whether the receptor localizes synaptically or extrasynaptically. By contrast, α4-containing synaptic and extrasynaptic receptors show different modulation by PKA and PKC phosphorylation. PKA activation decreases synaptic α4 expression while increases extrasynaptic α4. Activation of PKC instead promotes α4-expression at the synapse and has no effect extrasynaptically[56].

Dendritic spines are the postsynaptic sites where most excitatory synapsis occurs. Their change in number and morphology underlies synaptic plasticity, important for learning and memory processes. GABA, through $GABA_A$Rs activation promotes spine shrinkage and elimination[57]. Specifically, $GABA_A$Rs containing α4βδ subunits have been involved in synaptic pruning at the CA1 and CA3 regions in the hippocampus[27],[28]: the expression of the α4 subunit of $GABA_A$Rs increases in the hippocampus during adolescence[28] and the density of dendritic spines decreases post-pubertal, while in the *GABRA4* KO mice this pruning does not occur. Therefore, the density of dendritic spines in the hippocampus of adult mice is increased in the

*GABRA4* KO mice[37]. The effect of α4 on synaptic pruning is mainly observed in mushroom-
394 and stubby-shaped dendritic spines[27],[28]. According to a role of Ccnd1 in promoting α4-
containing $GABA_A$Rs activity, we observed an increase in the proportion of mushroom-type
396 spines in *CCND1* KO neurons. Mushroom spines are considered to be one of the mature types
of spines, involved in memory[58]. In this sense, the increase in α4βδ receptors at puberty
398 impairs learning[25] and the *GABRA4* KO mouse has increased spatial memory[37]. In the same
direction, increased expression of Ccnd1 was found in CA1 region of aged learning-impaired
400 rats[59] and the expression of Ccnd1 in the hippocampus of rats triggers deficits in spatial
working memory[60]. Moreover, *GABRA4* KO mice show an autistic-like behavior, and autism
402 has been associated with an increased number of spines[61]. The effect of Ccnd1 on GABA
signaling and dendritic spines opens the possibility of exploring Ccnd1 functions in diseases
404 related to the imbalance between inhibitory/excitatory signaling and dendritic spine
abnormalities such as autism spectrum disorders and epilepsy.

406

408 **MATERIALS and METHODS**

**Cell culture.** Mycoplasma-free HEK293T cells were obtained from the American Type Culture
410 Collection. Cells were maintained at 37ºC in a 5% $CO_2$ incubator, and grown in Dulbecco's
modified Eagle's medium (DMEM) supplemented with 10% Fetal Bovine Serum (FBS), 10 U/mL
412 penicillin/streptomycin (P/S) and 4 mM glutamine. Mycoplasma detection tests were
performed in the Cell culture service (SCT-CC). Transient transfection of vectors was performed
414 with Lipofectamine 2000 (Invitrogen) according to manufacturer's instructions.

**Expression vectors.** Human CCND1 was fused to three copies of the Flag or HA or one of Red
416 monomer epitope under the CMV promoter in pcDNA3. Ccnd1-CAAX construct is a fusion of
the 3' end of the K-Ras ORF containing the CAAX motif (GGC TGT GTG AAA ATT AAA AAA TGC
418 ATT ATA ATG TAA) to the 3' end of the CCND1 ORF[10]. Mouse GABRA4 (IMAGE ID 6828002,

Source BioScience) and Human GABRB3 (IMAGE ID 3871111, Source BioScience) were used to
420 obtain N-terminal GST fusions in pGEX-KG (Clontech) or N-terminal FLAG fusions in pJEN1 (pcDNA3 derived, from Dr. Egea) or cloned into FCIV1 lentiviral vector (from Dr. Encinas).
422 Standard PCR-mediated site-directed mutagenesis was used to obtain the non-phosphorylatable and phosphomimetic mutants of GABRA4 using the following primers: T423A
424 and S431A: CGCCAAATCCATTCAGCAGGGC and CCGAAGCTAAGTGAGCCTTAGGCGCGGCTTCAGAAGACTCCTGGAC; S456A and S458A:
426 CGGCCCCCGCTCCTCATGGCACATTGCGGC and CGGCAGATGAAAGACCTCTGGCTGM; T500A: CGCCTCCTCCCCCTGCTCCAC and CCGCTGACACATTCCCAGCAGC; and T423E and S431E:
428 GCGAACCAAATCCATTCAGCAGGGC and TAGCTAAGTGAGCCTTAGGCTCGGCTTCAGAAGACTCCTGGAC.

430 **Immunoprecipitation assays.** For co-immunoprecipitation experiments, HEK293T cells were harvested 24 h after transfection. The cells were resuspended in RIPA buffer (50mM Tris
432 pH7.4, 150mM NaCl, 1% NP-40, 0.1% sodium deoxycholate, 0.1% SDS, 5mM EDTA, protease and phosphatase inhibitors), rocked 1 h at 4ºC, and spun for 5 min at 600 g. The supernatants
434 were incubated with protein G magnetic beads (Dynabeads, Invitrogen) for 30' at 4ºC. After the preclearing, the samples were incubated with 2 µg of αFLAG M2 antibody (Sigma)
436 overnight and precipitated with protein G dynabeads. IP of anti-phosphoThreonineProline antibody (#9391, Cell Signaling) was performed similarly, but using protein A dynabeads. The
438 beads were collected and washed three times with 1 mL of cold RIPA buffer, and bound proteins were separated by SDS-PAGE gels and visualized by western blots.

440 IP of endogenous Ccnd1 was carried out in hippocampus of adult female mice with a polyclonal antibody (#06‑137, Upstate). Briefly, cleared cell extracts in RIPA buffer (with
442 protease and phosphatase inhibitors) were immunoprecipitated with Protein A linked to magnetic beads (Invitrogen). An anti-FLAG (#F7425, Sigma) was used as a mock control.
444 Washes were performed with RIPA buffer without SDS.

**Immunoblotting**. For immunoblot, protein samples were resolved by SDS-PAGE, transferred to
446 PVDF membranes (Millipore), and incubated with primary antibodies: anti-Ccnd1 (monoclonal DCS-6, BD biosciences, 1:500), anti-Gabra4 (polyclonal, AB5459, Merck, 1:1000, and polyclonal
448 12979-1-AP, Proteintech, 1:500), anti-Flag (polyclonal, 11508721, Invitrogen, 1:1000), anti-HA (rat monoclonal 3F10, Roche #11867431001, 1:5000), anti-TFR (monoclonal H68.4, Invitrogen
450 #13‑6800, 1:1,000) and anti-GST (goat polyclonal, Amersham #27‑4577, 1:2000). Appropriate peroxidase-linked secondary antibodies (GE Healthcare UK Ltd) were detected using the
452 chemiluminescent HRP substrate Immobilon Western (Millipore). Chemiluminescence was recorded with a ChemiDoc-MP imaging system (BioRad).

454 **Production and purification of recombinant proteins**. All of the GST fusions were expressed in *E. coli* BL21 (DE3) by adding 1 mM isopropyl-β-D-thiogalactopyranoside (IPTG) to LB broth
456 cultures at a cell density of 0.3 $A_{600}$ and subsequent incubation for 4 h at 30 °C. The proteins were purified using glutathione-Sepharose 4B beads as directed by the supplier (Amersham
458 Biosciences) in 500 µl of lysis buffer containing 50mM HEPES, pH 7.5, 150 mM NaCl, 1 mM EDTA, 0.5% Triton X-100, 10% glycerol, 1 mM DTT, and protease and phosphatase inhibitors.
460 The concentration and purity of substrates were estimated by comparison to protein standards stained with Coomassie Brilliant Blue.

462 For *in vitro* transcription and translation, FLAG-Ccnd1 was amplified by PCR (forward primer: CGCGCTAATACGACTCACTATAGGGAGACCCAAGCCCATGGGATCAC; reverse primer:
464 TTTTTTTTTTTTTTTTTTTTTTTTTTTTTTGGCTGATCAGCGAGCTCTAG), transcribed *in vitro* with the T7 RNA polymerase (New England Biolabs), and *in vitro* translated with a Rabbit Reticulocyte
466 Lysate system (Promega).

**GST pull-down assay**. For the GST pull-down assay, 400 ng of GST or GST-α4 or GST-Cter-α4
468 purified from *E. coli* immobilized on Glutathione-Sepharose 4B beads were incubated with Flag-Ccnd1 in binding buffer (20 mM HEPES-KOH, pH 7.5, 150 mM KCl, 5 mM $MgCl_2$, 0.5 mM
470 EDTA, 0.1% NP-40, 1 mM DTT, 1 mM PMSF, 10% glycerol, protease and phosphatase

inhibitors) for 30 min at room temperature. After four washes with the same buffer, the
472 samples were analyzed by SDS-PAGE.

**Kinase assay**. Briefly, 0.2 mg substrate (either GST-α4, GST-Cter-α4 or GST-β3) was mixed with
474 1.5 µL of active Ccnd1-Cdk4 complex purified from baculovirus (Sigma C0620), 10 mM ATP, 7 mCi of γ-$^{32}$P-ATP (PerkinElmer, 3000 Ci/mmol), and either DMSO or 2 µM of the Cdk4/6-
476 inhibitor Palbociclib (Selleckchem, S1116) in 20 µL of kinase buffer (50 mM Tris‑HCl pH 7.5, 10 mM $MgCl_2$, 0.5 mM DTT, 1 mM EGTA and 2.5 mM b-glycerophosphate). This mixture was
478 incubated for 20 min at 30 ºC, then boiled in 2x Laemmli buffer, and separated by electrophoresis. Phosphorylated proteins were visualized by autoradiography of the dried slab
480 gels.

**MS analysis of phosphopeptides**. The C terminus of α4 fused to GST was used in an *in vitro*
482 kinase assay with Ccnd1·Cdk4 in the presence of ATP or in the absence of ATP as a control. Samples were subsequently subjected to SDS-PAGE. The gels were stained with Coomassie
484 Brilliant Blue G-250 colloidal (EZBlue Gel Staining Reagent, Sigma). After washing with water, protein bands of interest were prepared and submitted to Fundació Institut d'Investigació
486 Biomèdica de Bellvitge (IDIBELL) Proteomics Service (Barcelona) for analysis of the Chymotryptic peptide molecular masses by liquid chromatography-mass spectrometry. Gel
488 slices were manually cut and proteomic service suggested for each band-assay to recover three slices (low 1, middle 2, and high 3 mobility) as phosphorylation could alter band mobility.
490 Briefly, gel bands were washed with water, ammonium bicarbonate (50mM) and 50% acetonitrile. Next, samples were reduced by incubation with DTT (10 mM) at 60 ºC for 45 min
492 and alkylated with iodoacetamide (50mM) for 30 min, in the dark. Finally, proteins were digested with chymotrypsin (5 ng/µL) at 25ºC overnight (Trypsin gold, Promega). Digestion was
494 stopped by addition of 5% formic acid and peptides extracted twice with 70% acetonitrile and 5% formic acid (10 min sonication). Peptide extracts were evaporated to dryness, resuspended
496 with 2% acetonitrile 0.1% formic acid and analyzed by nano-HPLC-MSMS.

**Surface biotinylation.** For surface biotinylation (all steps performed on ice) HEK-293T cells
498 were washed twice with PBS and incubated with 1 mg/mL EZ-link sulfo-NHS-SS-biotin (Pierce), a nonpermeable biotin, in PBS for 15 min. Following surface labeling, nonconjugated biotin
500 was quenched by washing twice with TBS. Cells were lysed in RIPA buffer (50 mM Tris, pH7.4, 150 mM NaCl, 1% NP-40, 0.1% SDS, 5 mM EDTA, with phosphatase and protease inhibitors),
502 and protein concentrations were determined using a DC protein assay (Bio-Rad). Equal amounts of protein (usually 1 mg in 500 µL) were incubated overnight with 20 µL NeutrAvidin-
504 coated beads (Pierce) at 4°C with constant rotation. The next day, beads were washed three times with RIPA buffer and eluted samples were processed for immunoblotting.

506 **Whole-cell currents measurements in tsA201 cells.** Electrophysiological experiments were done with mycoplasma-free tsA201 cells (kindly provided by Prof. F. Ciruela, Universitat de
508 Barcelona) and purchased from the American Type Culture Collection (ATCC, CRL-3216, RRID: CVCL_0063). Mycoplasma detection tests were performed with PlasmoTest (Invivogen, code:
510 rep-pt1). Cells were transiently co-transfected with 1 µg total cDNA using polyethylenimine (PEI) transfection reagent (1 mg/mL) in a 3:1 ratio (PEI:DNA). In all transfections the DNA ratio
512 used was 1:1:2 (plasmid A: plasmid B: plasmid C), where A is α4 or $\alpha4^{T423ES431E}$, B is β3 and C is a control vector or Ccnd1-CAAX codifying plasmid. Cells were re-plated on poly-D-lysine coated
514 glass coverslips to allow optimal density with isolated cells. All experiments were performed 48 h after transfection.

516 For the measurements of GABA-evoked whole-cell currents in tsA201, cells were visualized with an inverted microscope (AxioVert A.1, Carl Zeiss) and maintained in extracellular flowing
518 solution at a rate of 60 mL/h. The extracellular solution contained (in mM): 140 NaCl, 5 KCl, 10 HEPES, 11 glucose, 2.5 $CaCl_2$, 1.2 $MgCl_2$ (pH = 7.4 with NaOH; osmolarity 305 mOsm/Kg
520 adjusted with sorbitol). Electrodes were fabricated from borosilicate glass (1.50 mm O.D., 1.16 I.D., Harvard Apparatus) pulled with a P-97 horizontal puller (Sutter Instruments) and polished
522 with a forge (MF-830, Narishige) to a final resistance of 2–5 MΩ. The intracellular solution

contained (in mM): 140 KCl, 2 $MgCl_2$, 2 $CaCl_2$, 10 HEPES, 1.1 EGTA, 2 Mg ATP (pH = 7.2 with
524 KOH; osmolarity 295 mOsm/Kg adjusted with sorbitol).

Macroscopic $GABA_A$-mediated currents were recorded at room temperature (22-25˚C) in the
526 whole-cell configuration from cells positive for Venus (α4 in FCIV1) and mCherry (Ccnd1-CAAX in pcDNA3 Red monomer) fluorescence at a holding membrane potential of -60 mV. Currents
528 were recorded with Axopatch 200B amplifier, filtered at 2 kHz and digitized at 5 kHz using Digidata 1440A interface with pClamp 10 software (Molecular Devices Corporation). Series
530 resistance was typically 5–20 MΩ, and was monitored at the beginning and at the end of the experiment. Cells that showed a change in series resistance greater than 20% were rejected.

532 Rapid application of the agonist GABA (1-2 ms exchange) was applied by switching between a continuously flowing control solution (extracellular solution diluted by 5%) and a GABA-
534 containing solution (1 µM GABA and 2.5mg/mL of sucrose diluted in extracellular solution). Solution switching was achieved by piezoelectric translation of a theta-barrel application tool
536 made from borosilicate glass (1.5 mm O.D.; Sutter Instruments) mounted on a piezoelectric translator (P-601.30; Physik Instrumente). Agonist was applied at 2 minutes interval and the
538 magnitude of the peak current was measured ($I_{GABA}$). Electrophysiological recordings were analyzed using IGOR Pro (Wavemetrics Inc.) with NeuroMatic (Jason Rothman, UCL).

540 **Preparation of organotypic hippocampal slice cultures.** Organotypic hippocampal slice cultures were prepared as previously described[62]. Briefly, whole brain of newborn rats
542 (postnatal days 5-7) were dissected and placed in ice-cold $Ca^{2+}$-free dissection solution (10 mM D-glucose, 4 mM KCl, 26 mM $NaHCO_3$, 8% sucrose, 5 mM $MgCl_2$, 1:1000 Phenol Red) saturated
544 with 5% $CO_2$ / 95% $O_2$, enabling the brain to chill for 1 min. Hippocampi were then isolated with the help of a magnifying glass, cut in slices (400 µm) in the same solution using a tissue
546 chopper (Stoelting), and maintained at 35.5 °C in culture on permeable membranes in a medium containing 20% horse serum, 1 mM $CaCl_2$, 2 mM $MgSO_4$, 1 mg/L insulin, 0.0012%

548 ascorbic acid, 30 mM Hepes, 13 mM D-glucose, and 5.2 mM $NaHCO_3$. Culture medium was replaced with fresh one every 2-3 days. The slices were used at 4-8 days *in vitro*.

550 **Whole-cell recordings of $GABA_A$ receptor-mediated currents.** Prior to the electrophysiological recordings, slices were treated for 2 hours with either DMSO (control solution) or 2.5 µM 552 Palbociclib (Cdk4/6 inhibitor) (Selleckchem). After that, slices were placed in a chamber and perfused with artificial cerebrospinal fluid [aCSF: 119 mM NaCl, 2.5 mM KCl, 1 mM $NaH_2PO_4$, 554 26 mM $NaHCO_3$, 11 mM glucose, 1.2 mM $MgCl_2$, 2.5 mM $CaCl_2$; osmolarity adjusted to 290 mOsm; pH7.5] supplemented with 100 µM AP5 (NMDA receptor antagonist), 10 µM CNQX 556 (AMPA receptor antagonist), 1 µM strychnine (glycine receptor antagonist), 4 µM 2-chloroadenosine (to reduce neurotransmitter release and stabilize synaptic transmission) and 558 DMSO or Palbociclib as external solution gassed with 5% $CO_2$ / 95% $O_2$ at 29 °C in the electrophysiology set-up. Patch recording pipettes (4-6 MΩ) were pulled from thin-walled 560 borosilicate capillary glass (World Precision Instruments [WPI], Sarasota, FL) on a P-2000 laser electrode puller (Sutter Instrument, San Rafael, CA) and filled with high chloride internal 562 solution (178 mM CsCl, 10 mM Hepes, 2.5 mM $MgCl_2$, 4 mM $Na_2ATP$, 0.4 mM $Na_3GTP$, 10 mM sodium phosphocreatine, 0.6 mM EGTA; pH adjusted to 7.2, osmolarity adjusted to 290 564 mOsm). GABA inhibitory postsynaptic currents were evoked with single voltage pulses (200 µs, <30 V) delivered through platinum-iridium bipolar electrodes (FHC, Bowdoin, ME, USA) placed 566 on Schaffer collaterals. CA1 pyramidal neurons were recorded under whole-cell voltage-clamp at -60 mV using Multiclamp 700A amplifier (Molecular Devices, San Jose, CA, USA). At least 10 568 min of stable baseline synaptic responses and holding currents were recorded. The tonic $GABA_A$ receptor-mediated current was measured as the outward shift in holding current 570 following application of picrotoxin (100 µM). Synaptic responses were used to monitor effective inhibition of $GABA_A$Rs by picrotoxin. To measure miniature inhibitory postsynaptic 572 currents (mIPSC), 1 µM tetrodotoxin was added to the aCSF to block action potentials.

Recordings were obtained with the gap-free mode of pClamp and mIPSCs were analyzed with
574 the event detection of pCLAMP software (Molecular Devices).

**Cortical neuron culture.** For primary culture of cortical neurons, cortexes were dissected from
576 E15.5 *CCND1* KO or WT mice in ice-cold HBSS-MHPS (Hank's Balanced Salt Solution, 10 mM $MgSO_4$, 10 mM HEPES pH 7.2 and 10 U/mL P/S). After dissection, cortexes were incubated with
578 papain solution (1 mg/mL papain in HBSS-MHPS) at 37ºC for 23 min. Enzymatic digestion was inhibited by washing the tissue 3 times with 10 mg/mL trypsin inhibitor (Fisher) in HBSS-MHPS.
580 Additionally, one more wash was done with Neurobasal medium supplemented with 2% B27, 2 mM Glutamax and 1 mM sodium pyruvate (NB27, Fisher) at room temperature. The tissue was
582 triturated by passing it through a flame-polished Pasteur pipette (<20 times). After the mechanical disaggregation, the supernatant containing mostly single cells was centrifuged at
584 650 rpm for 4 min. The pellet was resuspended in NB27 and the cells were counted in a Neubauer chamber. Cells were seeded at low density (25000 cells/$cm^2$) with NB27 medium in
586 poly-D-lysine (0.5 mg/mL) and laminin (5 µg/mL)-coated plates, in 1:1 conditioned medium. One third of the culture medium is replaced with fresh one every 3-4 days. Primary cortical
588 neurons were transfected at 3 DIV using Lipofectamine 2000 (Invitrogen) following the manufacturer's recommendations and the proportion 0.3 µg DNA: 1.2 µL Lipofectamine2000.
590 The media was changed 4 hours after transfection and cells were fixed at 20 DIV.

**Genotyping of *CCND1* knockout mice.** *CCND1* knockout mice[12] were obtained from Charles-
592 River. Transgenic mice were maintained in a mixed background of C57BL/6 and SV129. Embryo's tails were collected and warmed at 95 ºC NaOH 50 mM for 45 min. After
594 neutralization with Tris 0.15 M pH8.5, the samples were then centrifuged for 1 minute at 10000 rpm. Supernatant containing genomic DNA was used for CCND1 genotyping by PCR. The
596 following primers were used: a common primer CTGTCGGCGCAGTAGCAGAGAGCTACAGAC, a CCND1 primer CGCACAGGTCTCCTCCGTCTTGAGCATGGC and a neomycin primer
598 CTAGTGAGACGTGCTACTTCCATTTGTCACG. PCR was performed in a Thermal Cycler (T100 Bio-

Rad) and PCR products were analyzed in a 1.5 % agarose gel followed by Ethidium Bromide
600 staining. The expected band pattern is 249 bp for WT, and 394 bp for KO alleles.

**Immunofluorescence and spine analysis**. Cortical neurons were fixed using 4% PFA and 4%
602 sucrose in PBS for 15 min at room temperature and then washed with PBS. Neurons were permeabilized for 5 min with 0.1% Triton X-100 in PBS and blocked with 3% BSA in PBS.
604 Primary antibody α-GFP (A11120, ThermoFisher) was diluted 1:200 in 0.3% BSA in PBS. Proteins were detected by incubation with secondary antibody Alexa 488 rabbit anti-mouse
606 (A11059, ThermoFisher). Images were acquired with an Olympus FV1000 confocal microscope using the following parameters: stacks of 10 slices were imaged every 0.37 µm, under a 60X
608 objective. Laser power and PMT values were kept constant throughout images and conditions. Immunofluorescence quantification was performed using NeuronJ of ImageJ. Spine density
610 and morphology analysis of WT and *CCND1* KO cortical neurons was performed on 3D reconstructions of confocal z series acquired using a 2x zoom. Spines were counted as
612 mushroom-type if the spine head was wider than the spine neck. All analysis was done blind to the experimental condition.

614 **Statistical analyses**. Different statistical analyses were used in this work. In every analysis, the minimum level of statistical significance was a p-value equal to 0.05. The significance level is
616 represented in each graph as indicated. In order to evaluate possible differences between two experimental groups a t-test was performed. When there was a multiple comparison, one-way
618 ANOVA with a post-hoc test (Tukey) was performed. In whole-cell recordings in ts201A cells, comparisons between groups were done using the parametric student's t-test. For tonic
620 currents comparison, Wilcoxon test was performed and in mIPSC amplitude, Mann-Whitney and Kolmogorov-Smirnov tests were done. Microsoft Excel and GraphPad Prism v5.0
622 (GraphPad) were used for statistical analysis and graphical representation.

**Ethical considerations.** All procedures with animals follow the protocols approved by the
624 Institutional Committee of Care and Use of Animals (Comitè Institucional de Cura i Ús

d'Animals), and experiments were approved by the Ethics Committee of the University of
626 Lleida (CEEA 03-02/19). Animals were housed and maintained in the animal facility of the University of Lleida with 12h:12h light/dark cycle and food/water available *ad libitum*. For
628 electrophysiological experiments, all biosafety procedures and animal care protocols were approved by the bioethics committee from the Consejo Superior de Investigaciones Cientificas
630 and were performed according to the guidelines set out in the European Community Council Directives (2010/63/EU, 86/609/EEC). All efforts were made to minimize the number of
632 animals and their suffering.

634 **COMPETING INTEREST STATEMENT**

The authors declared that they have no conflict of interest.

636

**ACKNOWLEDGEMENTS**

638 We are grateful to M. Encinas for plasmids. We thank Sònia Rius for technical assistance and members of the CYC lab for helpful considerations. The cell culture experiments were
640 performed in the Cell Culture Scientific & technical Service from Universitat de Lleida. This work was funded by the Spanish Ministry of Innovation and Science MICINN (PID2019-
642 104859GB-I00 to E.G. and PID2020-117651RB to J.A.E.) and by Generalitat de Catalunya (2017-SGR-569). M. Ventura Monserrat was supported by a predoctoral fellowship of University of
644 Lleida.

646 **AUTHORS CONTRIBUTION**

Neus Pedraza: conceptualization, supervision, validation, investigation, methodology, writing-
648 original draft, writing – review & editing; Ma Ventura Monserrat: validation, investigation, methodology; Francisco Ferrezuelo: funding acquisition, data curation, writing – review &
650 editing; Jordi Torres: funding acquisition, supervision, writing – review & editing; Neus

Colomina: funding acquisition, methodology; David Soto: funding acquisition, investigation, validation, methodology; Fede Miguez: investigation, methodology; JA Esteban: supervision, validation, methodology, funding acquisition; Joaquim Egea: funding acquisition, conceptualization, methodology; Eloi Garí: conceptualization, supervision, funding acquisition, investigation, writing – review & editing.

**REFERENCES**


1. Sherr CJ, Roberts JM. Living with or without cyclins and cyclin-dependent kinases. Genes Dev. 2004;18: 2699–2711. doi:10.1101/gad.1256504
2. Hydbring, Per, Malumbres M, Sicinski P. Non-canonical functions of cell cycle cyclins and cyclin-dependent kinases. Nat Publ Gr. 2016 [cited 17 Feb 2022]. doi:10.1038/nrm.2016.27
3. Neumeister P, Pixley FJ, Xiong Y, Xie H, Wu K, Ashton A, et al. Cyclin D1 Governs Adhesion and Motility of Macrophages. Mol Biol Cell. 2003;14. doi:10.1091/mbc.02-07-0102
4. Li Z, Wang C, Jiao X, Lu Y, Fu M, Quong AA, et al. Cyclin D1 Regulates Cellular Migration through the Inhibition of Thrombospondin 1 and ROCK Signaling. Mol Cell Biol. 2006;26: 4240–4256. doi:10.1128/mcb.02124-05
5. Cemeli T, Guasch-Vallés M, Nàger M, Felip I, Cambray S, Santacana M, et al. Cytoplasmic cyclin D1 regulates glioblastoma dissemination. J Pathol. 2019;248: 501–513. doi:10.1002/path.5277
6. Zhong Z, Yeow WS, Zou C, Wassell R, Wang C, Pestell RG, et al. Cyclin D1/cyclin-dependent kinase 4 interacts with filamin A and affects the migration and invasion potential of breast cancer cells. Cancer Res. 2010;70: 2105–2114. doi:10.1158/0008-5472.CAN-08-1108
7. Meng H, Tian L, Zhou J, Li Z, Jiao X, Li WW, et al. Cell Cycle PACSIN 2 represses cellular

migration through direct association with cyclin D1 but not its alternate splice form
678 cyclin D1b. Cell Cycle. 2011;10: 73–81. doi:10.4161/cc.10.1.14243
8. Fernández RMH, Ruiz-Miró M, Dolcet X, Aldea M, Garí E. Cyclin D1 interacts and
680 collaborates with Ral GTPases enhancing cell detachment and motility. Oncogene.
2011;30: 1936–1946. doi:10.1038/onc.2010.577
682 9. Fusté NP, Fernández-Hernández R, Cemeli T, Mirantes C, Pedraza N, Rafel M, et al.
Cytoplasmic cyclin D1 regulates cell invasion and metastasis through the
684 phosphorylation of paxillin. Nat Commun. 2016;7. doi:10.1038/ncomms11581
10. Fusté NP, Castelblanco E, Felip I, Santacana M, Fernández-Hernández R, Gatius S, et al.
686 Characterization of cytoplasmic cyclin D1 as a marker of invasiveness in cancer.
Oncotarget. 2016;7: 26979–26991. doi:10.18632/oncotarget.8876
688 11. Chen K, Jiao X, Ashton A, Rocco A Di, Pestell TG, Sun Y, et al. The membrane-associated
form of cyclin D1 enhances cellular invasion. Oncogenesis. 2020;9. doi:10.1038/s41389-
690 020-00266-y
12. Sicinski P, Donaher JL, Parker SB, Li T, Fazeli A, Gardner H, et al. Cyclin D1 provides a link
692 between development and oncogenesis in the retina and breast. Cell. 1995;82: 621–
630. doi:10.1016/0092-8674(95)90034-9
694 13. Lange C, Huttner WB, Calegari F. Cdk4/CyclinD1 Overexpression in Neural Stem Cells
Shortens G1, Delays Neurogenesis, and Promotes the Generation and Expansion of
696 Basal Progenitors. Cell Stem Cell. 2009;5: 320–331. doi:10.1016/j.stem.2009.05.026
14. Lim S, Kaldis P. Loss of Cdk2 and Cdk4 induces a switch from proliferation to
698 differentiation in neural stem cells. Stem Cells. 2012;30: 1509–1520.
doi:10.1002/stem.1114
700 15. Miyashita S, Owa T, Seto Y, Yamashita M, Aida S, Sone M, et al. Cyclin D1 controls
development of cerebellar granule cell progenitors through phosphorylation and
702 stabilization of ATOH1. EMBO J. 2021;40: 1–17. doi:10.15252/embj.2020105712

16. Sumrejkanchanakij P, Tamamori-Adachi M, Matsunaga Y, Eto K, Ikeda MA. Role of cyclin D1 cytoplasmic sequestration in the survival of postmitotic neurons. Oncogene. 2003;22: 8723–8730. doi:10.1038/sj.onc.1206870

17. Sumrejkanchanakij P, Eto K, Ikeda MA. Cytoplasmic sequestration of cyclin D1 associated with cell cycle withdrawal of neuroblastoma cells. Biochem Biophys Res Commun. 2006;340: 302–308. doi:10.1016/j.bbrc.2005.11.181

18. Marampon F, Casimiro M, Fu M, Powell M, Popov V, Lindsay J, et al. Nerve Growth factor regulation of cyclin D1 in PC12 cells through a p21RAS extracellular signal-regulated kinase pathway requires cooperative interactions between Sp1 and nuclear factor-kappaB. Mol Biol Cell. 2008;19: 2566–78. doi:10.1091/mbc.e06-12-1110

19. Schmetsdorf S, Gärtner U, Arendt T. Expression of cell cycle-related proteins in developing and adult mouse hippocampus. Int J Dev Neurosci. 2005;23: 101–112. doi:10.1016/j.ijdevneu.2004.07.019

20. Li C, Li X, Chen W, Yu S, Chen J, Wang H, et al. The different roles of cyclinD1-CDK4 in STP and mGluR-LTD during the postnatal development in mice hippocampus area CA1. BMC Dev Biol. 2007;7: 1–9. doi:10.1186/1471-213X-7-57

21. Nakamura Y, Darnieder LM, Deeb TZ, Moss SJ. Regulation of GABAARs by phosphorylation. Adv Pharmacol. 2015;72: 97–146. doi:10.1016/bs.apha.2014.11.008

22. Comenencia-Ortiz E, Moss SJ, Davies PA. Phosphorylation of GABA A receptors influences receptor trafficking and neurosteroid actions. Psycopharmacology. 2014;231: 3453–3465. doi:10.1007/s00213-014-3617-z

23. Chandra D, Jia F, Liang J, Peng Z, Suryanarayanan A, Werner DF, et al. GABAA receptor α4 subunits mediate extrasynaptic inhibition in thalamus and dentate gyrus and the action of gaboxadol. Proc Natl Acad Sci U S A. 2006;103: 15230–15235. doi:10.1073/pnas.0604304103

24. Shen H, Gong QH, Aoki C, Yuan M, Ruderman Y, Williams K, et al. Reversal of

neurosteroid effects at α4β2δ GABAA receptors triggers anxiety at puberty. Nat
730 Neurosci. 2007;10: 469–477. doi:10.1038/nn1868
25. Shen H, Sabaliauskas N, Sherpa A, Fenton AA, Aoki C, Smith SS. A Critical Role for α4βδ
732 GABAA Receptors in Shaping Learning Deficits at Puberty in Mice. Science (80- ).
2010;327: 1515–1518. doi:10.1126/science.1184245.A
734 26. Afroz S, Shen H, Smith SS. α4βδ GABAA receptors reduce dendritic spine density in CA1
hippocampus and impair relearning ability of adolescent female mice: Effects of a GABA
736 agonist and a stress steroid. Neuroscience. 2017;347: 22–35.
doi:10.1016/j.neuroscience.2017.01.051
738 27. Afroz S, Parato J, Shen H, Smith SS. Synaptic pruning in the female hippocampus is
triggered at puberty by extrasynaptic GABAA receptors on dendritic spines. Elife.
740 2016;5: 1–23. doi:10.7554/eLife.15106
28. Parato J, Shen H, Smith SS. α4βδ GABA A Receptors Trigger Synaptic Pruning and
742 Reduce Dendritic Length of Female Mouse CA3 Hippocampal Pyramidal Cells at
Puberty. Neuroscience. 2019;398: 23–36. doi:10.1016/j.neuroscience.2018.11.032
744 29. Shen H, Sabaliauskas N, Yang L, Aoki C, Smith SS. Role of α4-containing GABAA
receptors in limiting synaptic plasticity and spatial learning of female mice during the
746 pubertal period. Brain Res. 2017;1654: 116–122. doi:10.1016/j.brainres.2016.01.020
30. Moore MD, Cushman J, Chandra D, Homanics GE, Olsen RW, Fanselow MS. Trace and
748 contextual fear conditioning is enhanced in mice lacking the α4 subunit of the GABAA
receptor. Neurobiol Learn Mem. 2010;93: 383–387. doi:10.1016/j.nlm.2009.12.004
750 31. Duveau V, Laustela S, Barth L, Gianolini F, Vogt KE, Keist R, et al. Spatiotemporal
specificity of GABAA receptor-mediated regulation of adult hippocampal neurogenesis.
752 Eur J Neurosci. 2011;34: 362–373. doi:10.1111/j.1460-9568.2011.07782.x
32. Ma DQ, Whitehead PL, Menold MM, Martin ER, Ashley-Koch AE, Mei H, et al.
754 Identification of significant association and gene-gene interaction of GABA receptor

subunit genes in autism. Am J Hum Genet. 2005;77: 377–388. doi:10.1086/433195

33. Collins AL, Ma D, Whitehead PL, Martin ER, Wright HH, Abramson RK, et al. Investigation of autism and GABA receptor subunit genes in multiple ethnic groups. Neurogenetics. 2006;7: 167–174. doi:10.1007/s10048-006-0045-1

34. Griswold AJ, Van Booven D, Cuccaro ML, Haines JL, Gilbert JR, Pericak-Vance MA. Identification of rare noncoding sequence variants in gamma-aminobutyric acid A receptor, alpha 4 subunit in autism spectrum disorder. Neurogenetics. 2018;19: 17–26. doi:10.1007/s10048-017-0529-1

35. Fatemi SH, Reutiman TJ, Folsom TD, Rooney RJ, Patel H, Thuras PD. mRNA and Protein Levels for GABAAα4, α5, β1 and GABABR1 Receptors are Altered in Brains From Subjects With Autism. J Autism Dev Disord. 2010;40: 612–624. doi:10.1007/s10803-009-0924-z.mRNA

36. Fatemi S, Reutiman T, Folsom TD, Thuras PD. GABA A Receptor Downregulation in Brains of Subjects with Autism. J Autism Dev Disord. 2009;39: 223–230. doi:10.1007/s10803-008-0646-7

37. Fan C, Gao Y, Liang G, Huang L, Wang J, Yang X, et al. Transcriptomics of Gabra4 knockout mice reveals common NMDAR pathways underlying autism, memory, and epilepsy. Mol Autism. 2020;11: 1–17. doi:10.1186/s13229-020-0318-9

38. Ruiz-Miró M, Colomina N, Fernández RMH, Garí E, Gallego C, Aldea M. Translokin (Cep57) Interacts with Cyclin D1 and Prevents Its Nuclear Accumulation in Quiescent Fibroblasts. Traffic. 2011;12: 549–562. doi:10.1111/J.1600-0854.2011.01176.X

39. Abramian AM, Comenencia-Ortiz E, Vithlani M, Tretter EV, Sieghart W, Davies PA, et al. Protein kinase C phosphorylation regulates membrane insertion of GABA A receptor subtypes that mediate tonic inhibition. J Biol Chem. 2010;285: 41795–41805. doi:10.1074/jbc.M110.149229

40. Baker GL, Landis MW, Hinds PW. Multiple functions of D-type cyclins can antagonize

pRb-mediated suppression of proliferation. Cell Cycle. 2005;4: 329–337. doi:10.4161/cc.4.2.1485

41. Bright DP, Smart TG. Methods for recording and measuring tonic GABAA receptor-mediated inhibition. Front Neural Circuits. 2013;5: 193. doi:10.3389/fncir.2013.00193

42. Tang X, Hernandez CC, Macdonald RL. Modulation of spontaneous and GABA-evoked tonic α4β3δ and α4β3γ2L GABAA receptor currents by protein kinase A. J Neurophysiol. 2010;103: 1007–1019. doi:10.1152/jn.00801.2009

43. Connelly WM, Errington AC, Giovanni G Di, Crunelli V. Metabotropic regulation of extrasynaptic GABAA receptors. Front Neural Circuits. 2013;7: 1–8. doi:10.3389/fncir.2013.00171

44. Artegiani B, Lindemann D, Calegari F. Overexpression of cdk4 and cyclinD1 triggers greater expansion of neural stem cells in the adult mouse brain. J Exp Med. 2011;208: 937–948. doi:10.1084/jem.20102167

45. Yamada M, Takeshita T, Miura S, Murata K, Kimura Y, Ishii N, et al. Loss of hippocampal CA3 pyramidal neurons in mice lacking STAM1. Mol Cell Biol. 2001;21: 3807–19. doi:10.1128/MCB.21.11.3807-3819.2001

46. Fernández-Hernández R, Rafel M, Fusté NP, Aguayo RS, Casanova JM, Egea J, et al. Cell Cycle Cyclin D1 localizes in the cytoplasm of keratinocytes during skin differentiation and regulates cell-matrix adhesion) Cyclin D1 localizes in the cytoplasm of keratinocytes during skin differentiation and regulates cell-matrix adhesion. Cell Cycle. 2013;12: 2510–2517. doi:10.4161/cc.25590

47. Cajigas IJ, Tushev G, Will TJ, Tom Dieck S, Fuerst N, Schuman EM. The Local Transcriptome in the Synaptic Neuropil Revealed by Deep Sequencing and High-Resolution Imaging. Neuron. 2012;74: 453–466. doi:10.1016/j.neuron.2012.02.036

48. Stelzer A, Kay A, Wong R. GABAA-receptor function in hippocampal cells is maintained by phosphorylation factors. Science (80- ). 1988;241: 339–41.

doi:10.1126/science.2455347

808 49. Chen QX, Stelzer A, KAY AR, Wong RKS. GABAA receptor function is regulated by phosphorylation in acutely dissociated guinea-pig hippocampal neurones. J Physiol.
810 1990;420: 207–221.

50. Gyenes M, Wang Q, Gibbs TT, Farb DH. Phosphorylation factors control
812 neurotransmitter and neuromodulator actions at the gamma-aminobutyric acid type A receptor. Mol Pharmacol. 1994;46: 542–549.

814 51. Abramian AM, Comenencia-Ortiz E, Modgil A, Vien TN, Nakamura Y, Moore YE, et al. Neurosteroids promote phosphorylation and membrane insertion of extrasynaptic
816 GABAA receptors. Proc Natl Acad Sci U S A. 2014;111: 7132–7137. doi:10.1073/pnas.1403285111

818 52. Kittler JT, Chen G, Honing S, Bogdanov Y, McAinsh K, Arancibia-Carcamo IL, et al. Phospho-dependent binding of the clathrin AP2 adaptor complex to GABA A receptors
820 regulates the efficacy of inhibitory synaptic transmission. Proc Natl Acad Sci U S A. 2005;102: 14871–14876. doi:10.1073/pnas.0506653102

822 53. Gonzalez C, Moss SJ, Olsen RW. Ethanol promotes clathrin adaptor-mediated endocytosis via the intracellular domain of δ-containing GABAA receptors. J Neurosci.
824 2012;32: 17874–17881. doi:10.1523/JNEUROSCI.2535-12.2012

54. Bracamontes JR, Li P, Akk G, Steinbach JH. Mutations in the Main Cytoplasmic Loop of
826 the GABA A Receptor a 4 and d Subunits Have Opposite Effects on Surface Expression. Mol Pharmacol. 2014;86: 20–27. doi:10.1124/mol.114.092791

828 55. Wafford KA, Thompson SA, Thomas D, Sikela J, Wilcox AS, Whiting PJ. Functional Characterization of Human y-Aminobutyric AcidA Receptors Containing the a4 Subunit.
830 Mol Pharmacol. 1996.

56. Bohnsack JP, Carlson SL, Morrow AL. Differential regulation of synaptic and
832 extrasynaptic α4 GABA(A) receptor populations by protein kinase A and protein kinase

C in cultured cortical neurons. Neuropharmacology. 2016;105: 124–132. doi:10.1016/j.neuropharm.2016.01.009

57. Hayama T, Noguchi J, Watanabe S, Takahashi N, Hayashi-Takagi A, Ellis-Davies GCR, et al. GABA promotes the competitive selection of dendritic spines by controlling local Ca 2+ signaling. Nat Neurosci. 2013;16: 1409–1416. doi:10.1038/NN.3496

58. Bourne J, Harris KM. Do thin spines learn to be mushroom spines that remember? Curr Opin Neurobiol. 2007;17: 381–6. doi:10.1016/j.conb.2007.04.009

59. Burger C, López MC, Feller JA, Baker H V, Muzyczka N, Mandel RJ. Changes in transcription within the CA1 field of the hippocampus are associated with age-related spatial learning impairments. Neurobiol Learn Mem. 2007;87: 21–41. doi:10.1016/j.nlm.2006.05.003

60. Wu K, Li S, Bodhinathan K, Meyers C, Chen W, Campbell-Thompson M, et al. Enhanced expression of Pctk1, Tcf12 and Ccnd1 in hippocampus of rats: Impact on cognitive function, synaptic plasticity and pathology. Neurobiol Learn Mem. 2012;97: 69–80. doi:10.1016/j.nlm.2011.09.006

61. Penzes P, Cahill ME, Jones KA, VanLeeuwen J-E, Woolfrey KM. Dendritic spine pathology in neuropsychiatric disorders. Nat Neurosci. 2011;14: 285–93. doi:10.1038/nn.2741

62. Gähwiler B, Campogna M, Debanne D, McKinney R, Thompson S. Organotypic slice cultures: a technique has come of age. Trends Neurosci. 1997;20: 471–477. doi:10.1016/S0166-2236(97)01122-3

| Accession | Description | Score | Coverage | # Proteins | # Unique Peptides | # Peptides | MW (kDa) |
|---|---|---|---|---|---|---|---|
| Q9D6F4 | GBRA4_MOUSE | 309,37 | 33,70 | 1 | 16 | 17 | 60,8 |

| Sample | Peptide sequence | Modifications | phoSite Probab | q-Value | MH+ (Da) | ΔM (ppm) | RT (min) |
|---|---|---|---|---|---|---|---|
| ATP | TSAVQESSEATPK | | | 0,002 | 1334,64 | -1,09 | 15,99 |
| | TSAVQESSEA**t**PK | T11(Phospho) | T(11): 100,0 | 0,012 | 1414,61 | -1,91 | 15,92 |
| | AHLASSPNPFSR | | | 0,038 | 1283,64 | -3,28 | 19,81 |
| | AHLAS**s**PNPFSR | S6(Phospho) | S(6): 98,3 | 0,131 | 1363,61 | -5,17 | 20,50 |
| no ATP | TSAVQESSEATPK | | | 0,0000 | 1334,64 | -0,91 | 16,33 |
| | AHLASSPNPFSR | | | 0,0000 | 1283,64 | -3,57 | 20,01 |

***S1 Table. The α4 subunit of GABA$_A$ receptors is phosphorylated at T423 and S431 by Ccnd1·Cdk4.*** *The GST-Ct-α4 wild type was used in an in vitro kinase assay with Ccnd1·Cdk4, in the presence or absence of ATP, and the Chymotryptic peptide molecular masses were analyzed by liquid chromatography-mass spectrometry. MH+: proton adduct; ΔM: mass difference; RT: retention time; q-value: adjusted p-value. Both T423 and S431 of α4 subunit (highlighted in red) were found to be phosphorylated by Ccnd1·Cdk4.*

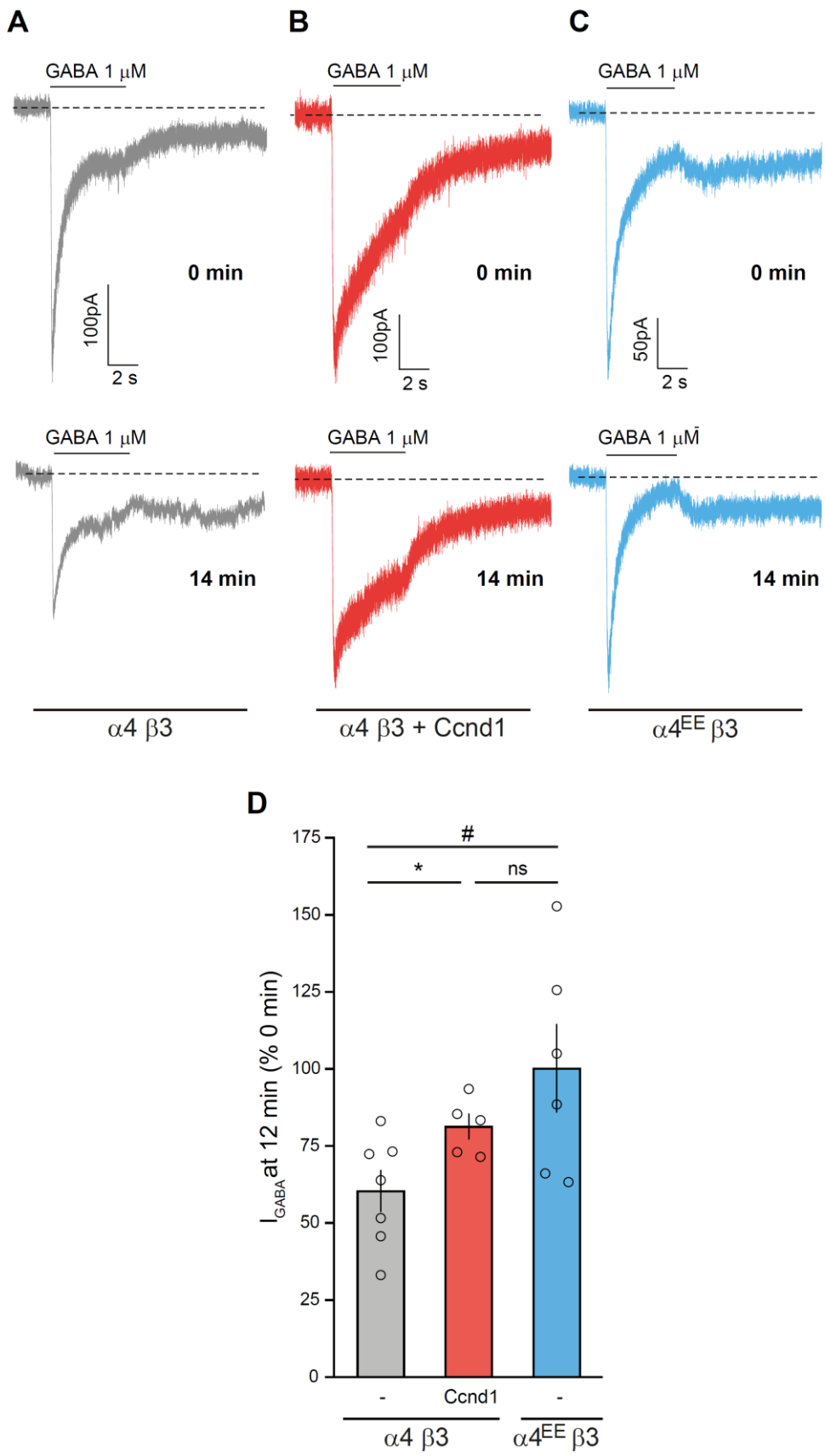
A
B
C
GABA 1 μM
0 min
14 min
100pA
50pA
2 s
α4 β3
α4 β3 + Ccnd1
α4EE β3
D
#
*
ns
175
150
125
100
75
50
25
0
IGABA at 12 min (% 0 min)
-
Ccnd1
-
α4 β3
α4EE β3

864

866 ***S1 Figure. Ccnd1 or the phosphomimetic allele of α4 ($α4^{EE}$) decreases $GABA_A$ receptor rundown.*** *A) Representative recording of whole-cell currents evoked by rapid application of 1 μM GABA (solid line*

868 *above the trace) to HEK-tsA201 cells expressing wild-type α4β3 $GABA_A$Rs. The GABA-evoked current at the beginning of the recording (time 0 min) and the response after 14 minutes (time 14 min) are shown.*

870 *Dashed line denotes the zero current. Holding potential was held at −60mV. B) Same as A, but from cells co-expressing wild-type α4β3 $GABA_A$Rs plus Ccnd1-CAAX. Note that the rundown of the peak current at*

872 *14 minutes is smaller than in condition A. C) Same as A, but from cells co-expressing phosphomimetic (T423E S431E) $GABA_A$ receptor $α4^{EE}β3$. D) Bar graph showing the mean ± S.E.M. of the relative current at*

874 *t=12 minutes compared with current at time=0 for cells expressing wild type α4β3 $GABA_A$Rs (n=7), α4β3 $GABA_A$Rs plus Ccnd1-CAAX (n=5) or for $α4^{EE}β3$ $GABA_A$Rs (n=6). Open circles denote single experimental*

876 *values. *p<0.05, α4β3 vs. α4β3+Ccnd1-CAAX; #p<0.05 α4β3 vs. $α4^{EE}β3$; Unpaired student's t-Test.*

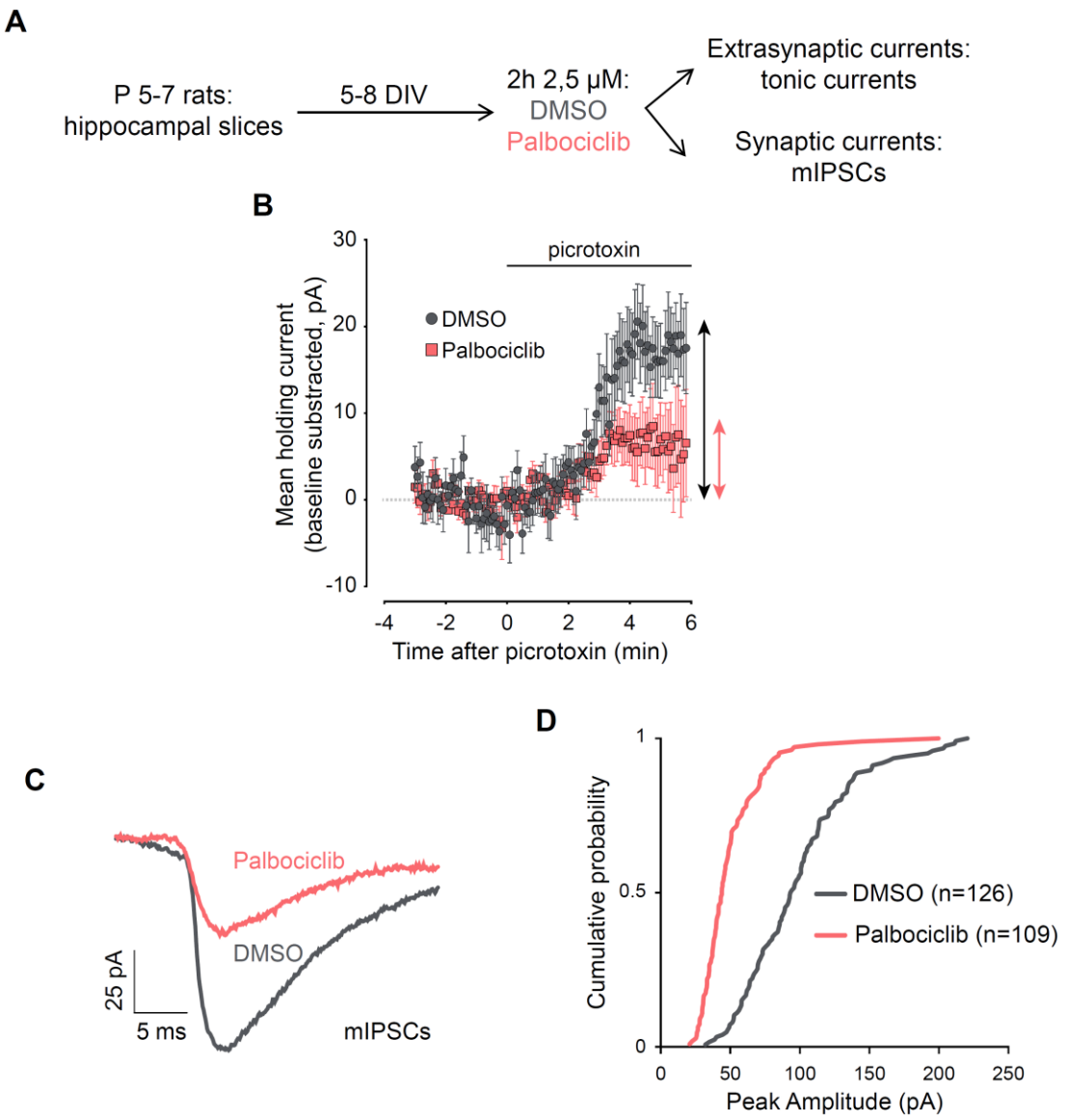


878

***S2 Figure. Cdk4/6 inhibition by Palbociclib decreases GABA tonic currents and mIPSC amplitude in rat***

880 ***hippocampal slices.*** *A) Schematic representation of the experimental design for GABA currents recordings in CA1 neurons: hippocampal slices from newborn rats were cultured in vitro, treated for 2 h*

882 *with DMSO or Palbociclib 2.5 µM, and tonic (extrasynaptic) or mIPSCs (synaptic currents) were measured. B) GABA inhibitory postsynaptic currents were evoked by stimulation of Schaffer collaterals*

884 *and the tonic $GABA_A$ receptor-mediated current was measured as the outward shift in holding current following application of the $GABA_AR$ antagonist picrotoxin. CA1 pyramidal neurons were recorded under*

886 *whole-cell voltage-clamp at -60 mV. Effects of picrotoxin (100 µM) on holding currents recorded in*

*DMSO- (grey rounds) or Palbociclib-treated (red squares) hippocampal slices are represented: the shift in*
888 *holding currents is shown as double-headed arrows for DMSO (grey) and Palbociclib (red). Recordings*
*are aligned at the time of picrotoxin addition (t=0). Each point represents the mean value of holding*
890 *current at a specific time for 10 cells. C) To measure miniature inhibitory postsynaptic currents (mIPSC), 1*
*µM tetrodotoxin was added to block action potentials. Representative traces of mIPSC of DMSO- or*
892 *Palbociclib-treated cells are shown. E) Cumulative distribution of mIPSC amplitude from CA1 pyramidal*
*neurons treated with either Palbociclib or control vehicle, as indicated. "n" represents number of*
894 *miniature responses recorded from nine (DMSO) or eight (Palbociclib) cells. (*p<0.001, Kolmogorov-*
*Smirnov test).*

896

898

900

902

904

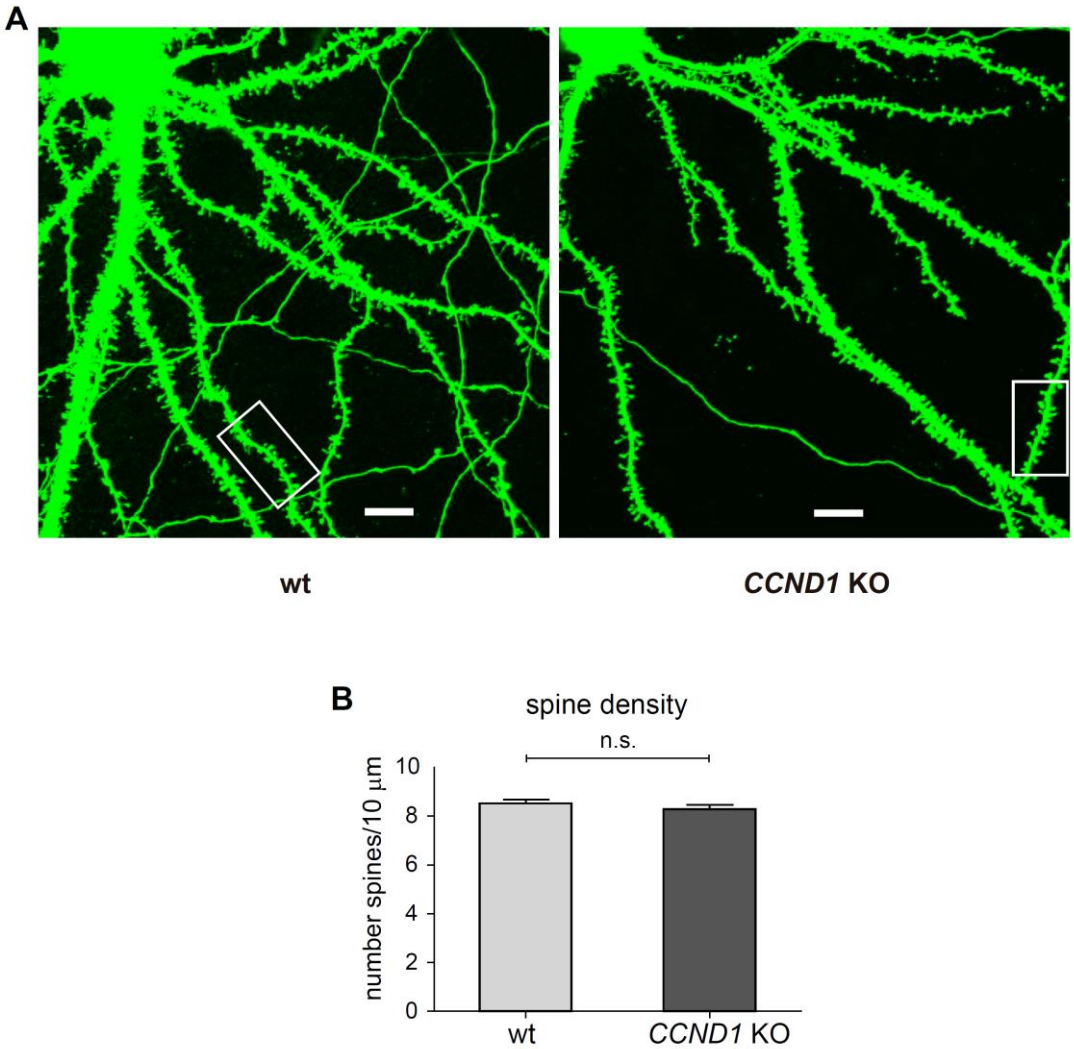


906

***S3 Figure. CCND1 KO increases the maturity of dendritic spines in cortical neurons****. A) Dendritic spine*

908 *analysis of WT and CCND1 KO mice cortical neurons at 20 DIV. Cultured cortical neurons were*

*transfected at 3 DIV with GFP and fixed at 20 DIV. Representative confocal images of WT and CCND1 KO*

910 *neurons. Scale bar: 10 µm. Changes in spine density and morphology were assessed by analyzing GFP-*

*positive neurons with NeuronJ (see Materials and Methods). B) Quantification of the number of total*

912 *dendritic spines relative to 10 µm of neurite, from WT (n= 59 neurons) and CCND1 KO (n= 62) neurons (4*

*mice/group). Bars show mean values ± S.E.M. ns: non-significant, Unpaired student's t-test.*

914